Journal of Geography, Environment and Earth Science International

Volume 28, Issue 3, Page 1-30, 2024; Article no.JGEESI.113182
ISSN: 2454-7352

Geospatial Variability and Distribution of Total Petroleum Hydrocarbons (TPH) in Soot-Contaminated Rain and Rivers at Oyigbo, Niger Delta, Nigeria

Nurudeen Onomhoale Ahmed [a*], Andrew Adesola Obafemi [b] and Godwin J. Udom [c]

[a] Institute of Natural Resources, Environment and Sustainable Development (INRES). University of Port Harcourt, Rivers State, Nigeria.
[b] Department of Geography and Environmental Management, Faculty of Social Sciences. University of Port Harcourt, Rivers State, Nigeria.
[c] Department of Geology, Faculty of Science. University of Port Harcourt, Rivers State, Nigeria.

Authors' contributions

This work was carried out in collaboration among all authors. All authors read and approved the final manuscript.

Article Information

DOI: 10.9734/JGEESI/2024/v28i3753

Open Peer Review History:
This journal follows the Advanced Open Peer Review policy. Identity of the Reviewers, Editor(s) and additional Reviewers, peer review comments, different versions of the manuscript, comments of the editors, etc are available here: https://www.sdiarticle5.com/review-history/113182

Original Research Article

Received: 16/12/2023
Accepted: 22/02/2024
Published: 27/02/2024

ABSTRACT

This comprehensive study delves into the analysis of Total Petroleum Hydrocarbon (TPH) concentrations in soot-contaminated rain and rivers within Oyigbo, Rivers State, Niger Delta, Nigeria, with a primary focus on unraveling the geospatial variability and distribution of TPH in the impacted water sources. The study adopts a multifaceted methodology, incorporating fieldwork, sampling, laboratory analysis, and geospatial mapping using ArcGIS 10.4 software to elucidate spatial variations. Results spotlight the highest rainwater TPH concentrations at MKT 7 - Umuosi

**Corresponding author: E-mail: nurudeenonomhoale@gmail.com;*

Market (128.179 mg/L) and the lowest at SET 13 - Okpontu Settlements (8.976 mg/L), situated in the Okoloma and Umu Agbai-Obete axis, respectively. Likewise, river water exhibits the highest TPH at RVR 5 - Imo River (37.118 mg/L), and the lowest at RVR 6 - Imo River (187.118 mg/L), at Okoloma and Umu Agbai-Obete axis. Analysis of the 41 samples indicates that 19 locations surpass the 50 mg/L acceptable limits set by the World Health Organization (WHO, 2017), and the Department of Petroleum Resources (DRP - EGASPIN, 2018), Nigeria standards, with 10 locations recording concentrations above, and 12 locations falling below 30 mg/L. These findings underscore approximately 46% exhibiting high, 24% displaying medium, and 29 % showcasing low concentrations across the study area, following a spatial pattern with higher pollution dispersion in the Northern and North-western regions at Okoloma and Obigbo axes, and lower pollution levels in the Eastern regions at Umu Agbai-Obete axis. In essence, this study provides a comprehensive insight into TPH in soot-contaminated water resources in Oyigbo, contributing significantly to the advancement of knowledge regarding spatial variation, distribution, and implications for water quality management. Furthermore, it serves as a valuable resource for policy development, offering evidence for targeted environmental programs and practical assistance to environmentalists, researchers, government agencies, and the public in the assessment and enhancement of water quality in affected communities.

Keywords: Atmospheric soot; water contamination; TPH distribution; geospatial variability; Oyigbo; Niger Delta; Nigeria.

1. INTRODUCTION

Water, as a fundamental resource, plays a pivotal role in sustaining life and serves various purposes such as agriculture, domestic use, industrial processes, and recreation [1]. Its quality is not only crucial for direct human consumption but is also integral to ecosystem services. In regions like the Niger Delta, the nexus between water availability, distribution, and spatial variation is particularly significant due to the challenges posed by factors such as population growth and industrialization [2,3].

The quality of the environmental system including surface, groundwater and soils is influenced by a myriad of factors, including both natural processes and human activities [4,5]. In petroleum-producing areas like the Niger Delta, oil-related activities, such as gas flaring, contribute to environmental pollution [6,7]. Gas flaring, a common practice in the region, releases pollutants like soot into the atmosphere, impacting air quality and subsequently affecting rainwater composition [8,9]. Rainfall, acting as a natural cleansing process, collects pollutants from the atmospheande, including total petroleum hydrocarbons (TPH) [10]. Soot, a byproduct of petroleum activities, poses health and environmental risks, affecting air and water quality [11].

Rainwater, a critical component of the hydrological cycle, serves as a pathway for pollutants present in the atmosphere, leading to the contamination of water resources [12,13]. In areas with extensive oil and gas activities, the introduction of soot and other pollutants poses health and environmental risks [14]. Therefore, understanding the geospatial distribution and variability of total petroleum hydrocarbons (TPH) in soot-contaminated rain and river water is imperative for assessing water quality in regions like Oyigbo, Rivers State, Niger Delta, Nigeria.

Soot, generated from petroleum hydrocarbon production and fossil fuel burning, is a significant anthropogenic pollutant with adverse effects on human health, visibility, ecosystems, agricultural productivity, and global warming [15]. Soot, a component of particulate matter, contains TPH, which is harmful to human health and the environment [16]. The presence of TPH, encompassing various petroleum hydrocarbons, adds complexity to the pollution landscape [17,6]. TPH includes potentially carcinogenic materials, particularly polycyclic aromatic hydrocarbons (PAHs), which are of concern due to their health implications [18].

The study aims to comprehensively assess the TPH concentrations in soot-contaminated rain and rivers at Oyigbo, Rives State, Niger Delta, Nigeria. It focuses on the geospatial variability and distribution of TPH in the soot-contaminated rain and river water. The Aliphatic Hydrocarbon and Polycyclic Aromatic Hydrocarbon concentrations were analyzed to assess the contamination status of surface and rainwater, providing insights into pollution hotspots and vulnerability areas.

In conclusion, understanding the geospatial distribution of TPH in soot-contaminated water resources is vital for sustainable water management in petroleum-producing areas. This research is crucial for water quality management, disease prevention, and environmental risk mitigation in the region. This study contributes valuable information to environmentalists, researchers, government agencies, and the public, aiding in the development of programs to assess and improve water quality in affected communities.

1.1 Study Area Description

1.1.2 Human geography of study area

Oyigbo, situated in the Niger Delta region of Nigeria, is both a town and a Local Government Area in Rivers State. This satellite town is strategically positioned approximately 30 kilometers northeast of Port Harcourt, falling within the geographic coordinates of latitude 4˚54' to 4˚46' N and longitude 7˚15' to 7˚25' W. Encompassing a total area of 248.00 km² (95.75 sq mi) (Fig. 1), Oyigbo plays a significant role in the regional landscape of Rivers State. Established in 1991, Oyigbo Local Government Area has its administrative headquarters located in Afam, commonly referred to as Okoloma-Ndoki. This administrative unit was carved out of Khana/Oyigbo Local Government in Rivers State. Oyigbo shares its boundaries with Khana to the Southeast, Tai to the South, Eleme and Obio/Akpor to the Southwest, while the entire Northern part is bounded by Abia State. The geographical composition of Oyigbo is characterized by its division into two distinct zones or regions, primarily inhabited by the Asa and Ndoki people [19]. This local government area occupies a pivotal position in the sociopolitical and economic dynamics of Rivers State, contributing to the diverse cultural and environmental tapestry of the Niger Delta region.

Rivers State, a prominent state in the Niger Delta region of Nigeria, is geographically surrounded by Imo State to the North, Delta State to the North-west, Akwa Ibom to the South-east, Abia State to the East, and Bayelsa State to the South-west. This strategic location places Rivers State at the heart of the Niger Delta, a region characterized by its rich cultural diversity and a mosaic of numerous ethnic groups. Within Rivers State, the Oyigbo area stands out as a hub of ethnic vibrancy, with various communities representing ethnicities such as Ekpeye, Andoni, Ikwerre, Ndoni, and the Ogoni. Among these groups, the Ikwerre people are the predominant ethnic community in the Oyigbo area [19].

The towns and communities within the Oyigbo Local Government Area are outlined in Table 1, depicting the varied regions that constitute this dynamic part of Rivers State. The population trends over the years, as highlighted in Table 2, reveal a notable increase from 40,407 in 1975 to 125,666 in 2015. This demographic surge is accompanied by a rise in population density, escalating from 163.1 km² in 1975 to 507.3 km² in 2015. The demographic dynamics of the Oyigbo area are intricately linked to the abundance of dry land and the unique terrain of the region. The population distribution in 2015 is further delineated, with 63,575 males and 62,091 females contributing to the vibrant demographic landscape of Oyigbo. This data provides a comprehensive snapshot of the population growth and composition, shedding light on the socio-economic and environmental factors shaping the Oyigbo area within the broader context of Rivers State [20].

1.2 Physical Geography of Study Area

The Oyigbo area is characterized by a tropical wet climate, with prolonged and intense rainy seasons and brief dry seasons. The dry season is confined to the months of November, December, January, and February. While the harmattan, a significant climatic feature in West Africa, has a milder impact on Oyigbo compared to other regions, the area experiences its heaviest precipitation in September, with an average of 370 mm of rain. Conversely, December stands out as the driest month, witnessing an average rainfall of 20 mm [21]. Temperature variations are minimal throughout the year, with average temperatures ranging between 25°C and 28°C. The hottest months span from February to May, featuring a marginal temperature difference of 2°C between these months. Relative humidity averages around 80 percent during the rainy season and drops to approximately 40 percent in the dry season, with high humidity prevailing for 8-10 months (March to November) and sometimes persisting throughout the year [21].

Situated in the equatorial rainforest belt of Nigeria, Oyigbo experiences a monthly mean temperature ranging from 25 to 28.5°C and an annual mean rainfall of about 2500 mm, with the majority occurring between May and October

[22,23] (Fig. 2). The rainfall distribution pattern showcases two lows in November and December and a second minimum in August, linked to the August break. From February to June and July, total rainfall rises steeply, reaching the primary maximum, followed by a second high in September and a decrease in November and December [22]. (Fig. 3 and 4). The dominant vegetation in the area comprises tropical rainforest or riparian vegetation, particularly along the river systems, and secondary bush resulting from farming or fallowing. The forest includes a first canopy with plants exceeding 40 meters, a middle canopy ranging from 15 to 40 meters, and mangrove shrubs reaching approximately 15 meters [21].

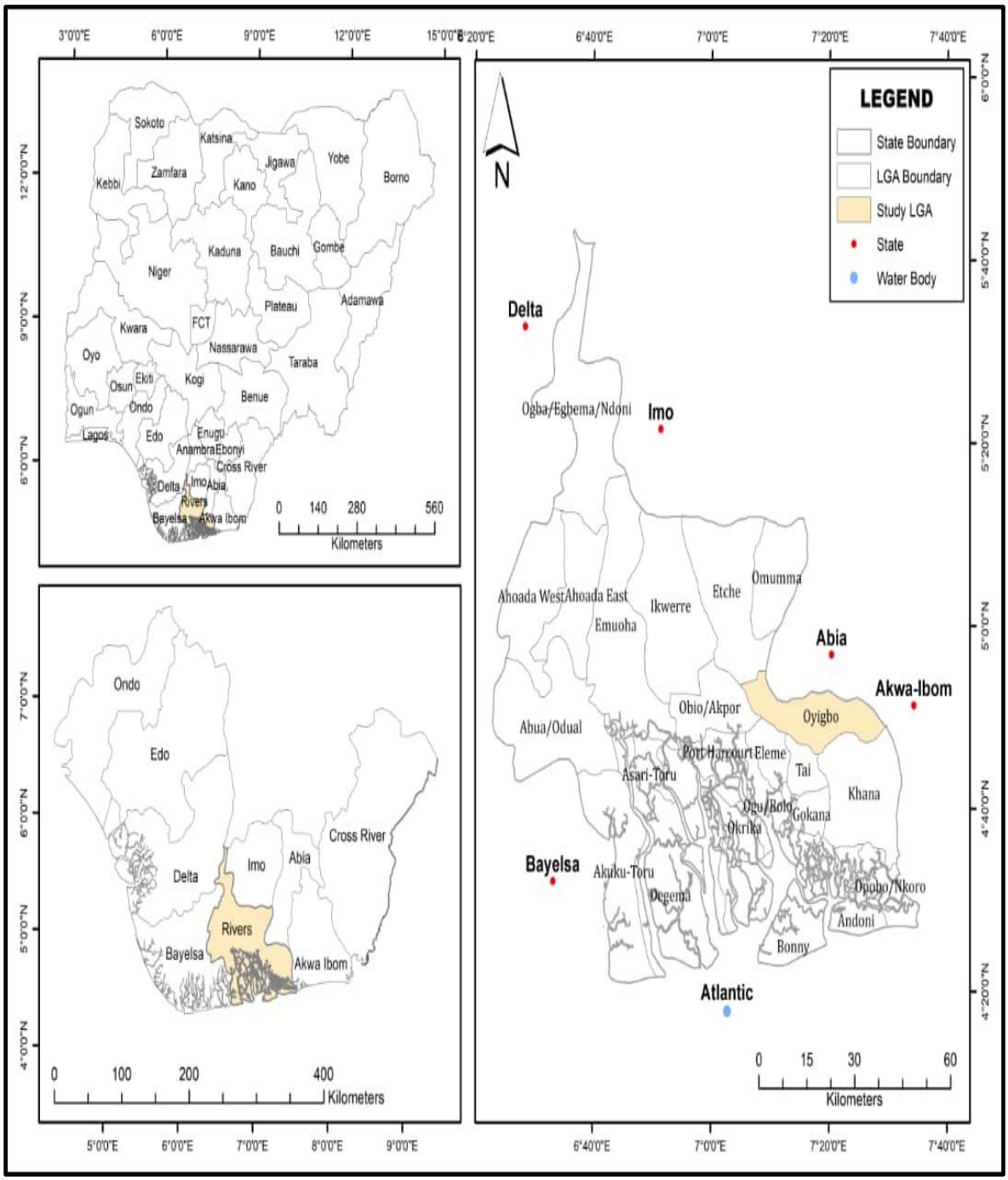

Fig. 1. Map of rivers state showing the study area
(Source: Digitized by Author)

Table 1. Towns/Communities of Oyigbo L.G.A. Zones/Regions

S/No	Asa Region / District / Zone	Ndoki Region / District / Zone
1	Obigbo	Afam Uku
2	Kom Kom	Afam Nta
3	Izuoma	Ayama
4	Obeama	Azuogu
5	Nmirinwayi	Egberu
6		Mgboji
7		Marihu
8		Obeakpu
9		Obete
10		Obunku
11		Okoloma
12		Okpontu
13		Umuagbai
14		Umuosi

Table 2. Population of Oyigbo from 1975 to 2015

Data	1975	1990	2000	2015
S/N	1	2	3	4
Population	40,407	63,533	82,697	125,666
Population Density	163.1/km^2	256.5/km^2	333.9/km^2	507.3/km^2

Source: NPC, 2006

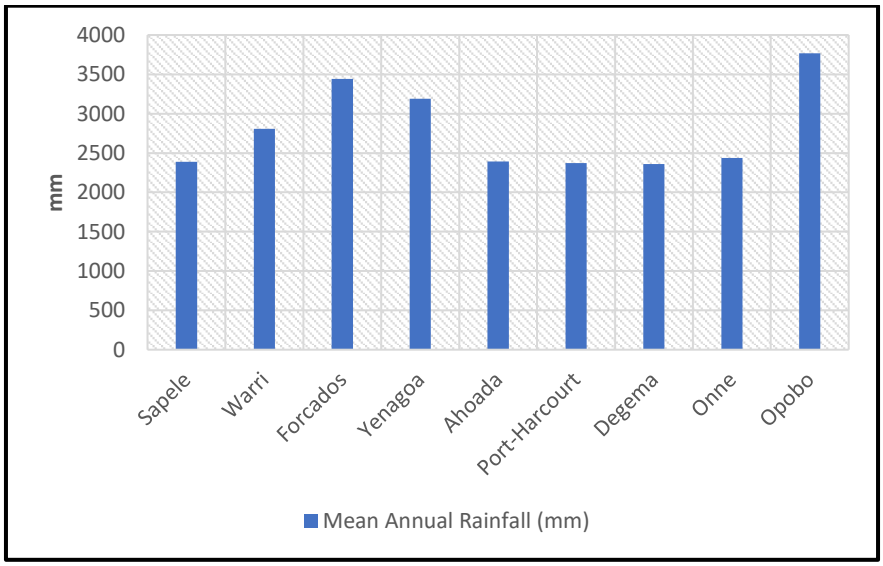

Fig. 2. Mean annual rainfall for Niger Delta
(Source: Adejuwon et al., [22])

The area boasts a rich variety of plants, including economic, medicinal, and food crops like palm trees and raffia palms. Originally abundant in economic trees, especially oil palms, the riverine areas feature freshwater swamp trees, palms, shrubs, and mangroves in beach ridge zones and tidal flats [24]. The topography of Oyigbo is characterized by sub-horizontal and gently sloping terrain. The wind predominantly blows from the South-West to North-West, with South-West being the most forceful direction [25]. Rainfall occurs for approximately ten months a year, with varying intervals. The region exhibits poor drainage due to a combination of low relief, high water table, and high rainfall, resulting in seasonally flooded Local Government Areas (LGAs) that impact agriculture and development activities.

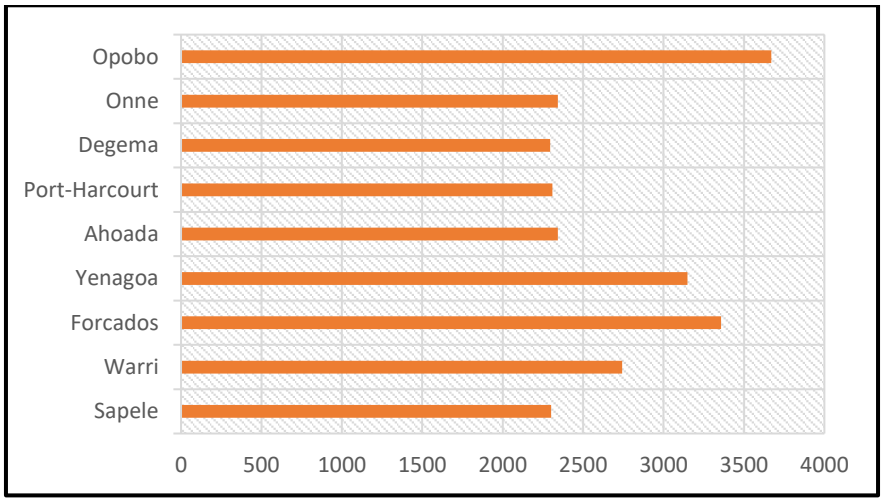

Fig. 3. Wet season rainfall amount (Feb/Mar-Nov) for Niger Delta
(Source: Adejuwon et al., [22])

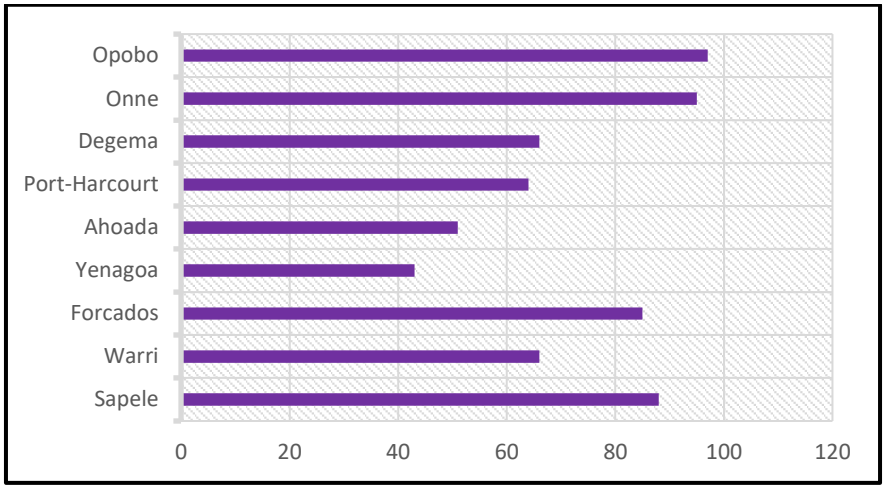

Fig. 4. Dry season rainfall amount (Dec-Jan/Feb) for Niger Delta
(Source: Adejuwon et al., [22])

The coastal plain, with an elevation of about 139m above sea level, comprises low-lying plains, swamps, creeks, and waterways. The land surface gently slopes (3-5 degrees on average) in the northwest to southeast direction [26]. The most significant water resource in Oyigbo L.G.A. is the Imo River, originating in Umuaku village and flowing through Abia, Imo, Rivers, and Akwa Ibom states. The Imo River, with three main tributaries (Aba River, Otamiri River, and Oramirukwa River), empties into the Atlantic Ocean through wide estuaries in Rivers State. The Imo River's estuary, approximately 40km wide, has an average discharge of 4000m3/s and encompasses 26,000 hectares of wetland. This vital water source supports the daily activities of communities along its banks and tributaries [27].

2. METHODOLOGY

2.1 Fieldwork and Sampling

The research involved the analysis of a total of 41 water samples, comprising 34 rainwater samples and 7 surface water samples. Fig. 5 and Table 3 provide details on the locations and specific points from which the rain and river water samples were collected. Rainwater collection was conducted directly as precipitation occurred, employing a purpose-built rainwater harvesting system consisting of receptor bottles with large funnel-tops. These rain harvesting apparatuses were strategically mounted on power grid poles to ensure a random yet uniform distribution across the study area. All utilized bottles underwent pre-sterilization. The collected

rainwater was then transferred from the receptor bottles to 1.5-liter plastic water sampling containers. In parallel, surface water samples were directly obtained from community rivers within the study area. The communities and locations were categorized into five study axes: Obigbo, Komkom-Obiama, Okoloma, Egberu, and Umu Agbai-Obete, to facilitate the sampling and identification processes. Geo-referencing of all sampling points was accomplished using the Garmin eTrex 32x, a rugged Handheld Global Positioning System (GPS). Additionally, on-site visual field observations were conducted and diligently recorded in the field notebook. A camera was employed to capture photographic evidence of crucial features and activities that could potentially serve as primary sources of water pollutants. This multifaceted approach aimed to ensure a thorough and well-documented sampling process for subsequent analysis in the laboratory. The fieldwork was conducted during the last quarter of 2021 and the first quarter of 2022.

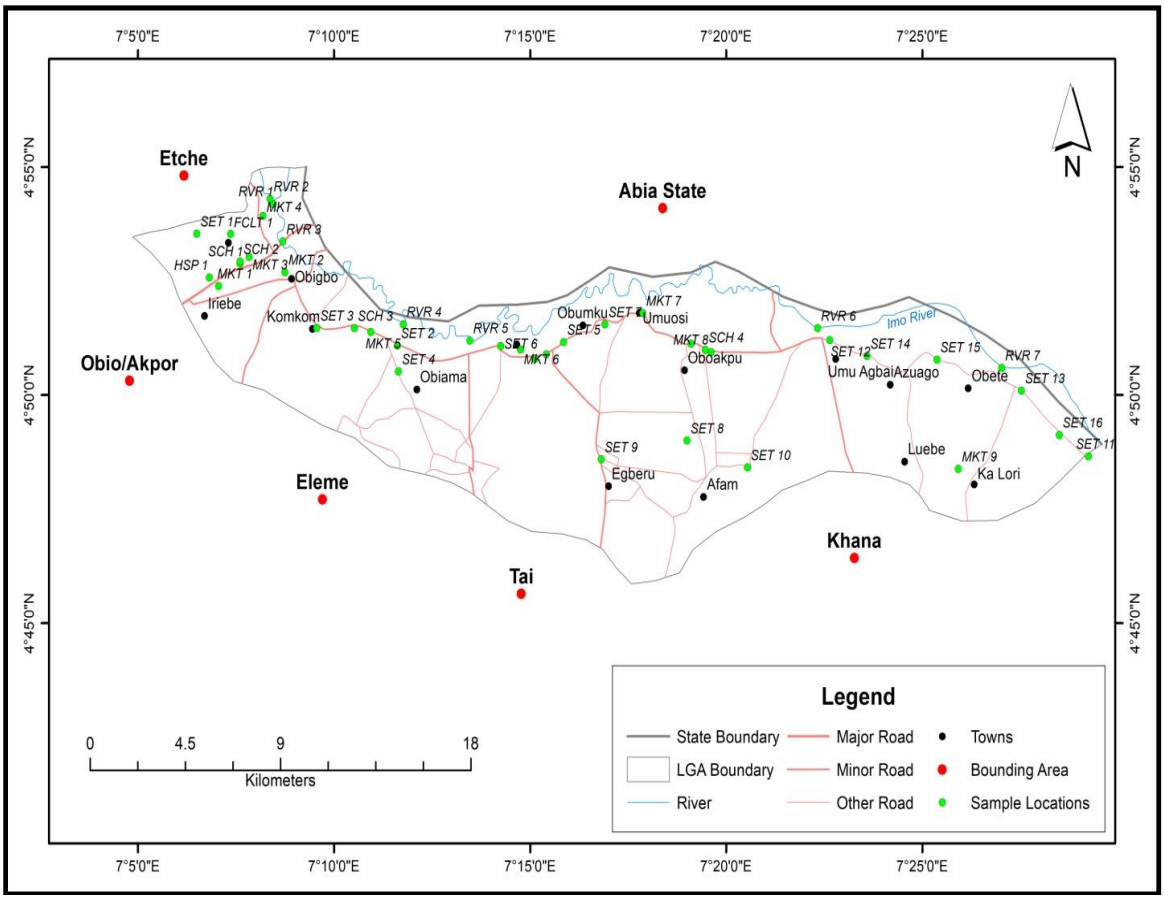

Fig. 5. Sampling points for the study area
(Source: Digitized by Author)

Table 3. Rain and river water sample location points

Sample Number	Study Axis	Sample Location	Sample Type	Sample ID	Coordinates	
					Latitude (N)	Longitude (E)
SN 1		Model Primary Health Care Centre	Rain	HSP 1	4° 52' 34.7984"	7° 06' 48.9204"
SN 2		Timber Market	Rain	MKT 1	4° 52' 23.4361"	7° 07' 03.3718"
SN 3	**Obigbo**	Obigbo Main Market	Rain	MKT 2	4° 52' 41.7036"	7° 08' 44.7853"

Sample Number	Study Axis	Sample Location	Sample Type	Sample ID	Coordinates	
					Latitude (N)	Longitude (E)
SN 4		Atata Market / Express Bus Stop Area	Rain	MKT 3	4° 53' 01.5396"	7° 07' 50.0344"
SN 5		Umuebele Market	Rain	MKT 4	4° 53' 55.7502"	7° 08' 11.1926"
SN 6		Community Secondary School, Umundinor	Rain	SCH 1	4° 52' 53.0860"	7° 07' 36.2982"
SN 7		Community Secondary School, Umuakpahu	Rain	SCH 2	4° 52' 55.8332"	7° 07' 36.0624"
SN 8		Oasis of Love Orphanage Settlement	Rain	SET 1	4° 53' 32.2656"	7° 06' 29.9628"
SN 9		Shell Flow Station Umuebele 4	Rain	FCLT 1	4° 53' 31.9279"	7° 07' 21.5270"
SN 10		Otamiri River – Umuebele 1	River	RVR 1	4° 54' 11.6281"	7° 08' 26.3642"
SN 11		Otamiri River – Umuebele 2	River	RVR 2	4° 54' 18.2052"	7° 08' 22.0704"
SN 12		Imo River – Obigbo/Abia Bridge	River	RVR 3	4° 53' 22.0646"	7° 08' 41.4646"
SN 13	**Komkom-Obiama**	Konko Market	Rain	MKT 5	4° 51' 22.8564"	7° 10' 56.0604"
SN 14		Community Secondary School, Komkom	Rain	SCH 3	4° 51' 28.0440"	7° 10' 31.0296"
SN 15		Lekuma-Obiama Settlement	Rain	SET 2	4° 51' 05.1120"	7° 11' 36.7692"
SN 16		Komkom Settlement	Rain	SET 3	4° 51' 28.2340"	7° 09' 33.6122"
SN 17		Obiama Settlement	Rain	SET 4	4° 50' 30.9264"	7° 11' 38.3784"
SN 18		Imo River – Obiama	River	RVR 4	4° 51' 33.1020"	7° 11' 45.8196"
SN 19	**Okoloma**	Okoloma Market	Rain	MKT 6	4° 50' 59.6040"	7° 14' 45.1680"
SN 20		Umuosi Market	Rain	MKT 7	4° 51' 47.6820"	7° 17' 52.4328"
SN 21		Ayama Settlement	Rain	SET 5	4° 51' 09.7200"	7° 15' 51.0840"
SN 22		Afam Settlement / Roundabout Area	Rain	SET 6	4° 51' 04.5000"	7° 14' 15.0360"
SN 23		Obumku Settlement	Rain	SET 7	4° 51' 33.0120"	7° 16' 54.4080"
SN 24		Okoloma Gas Plant	Rain	FCLT 2	4° 50' 40.2182"	7° 15' 12.6145"
SN 25		Afam Power Plant	Rain	FCLT 3	4° 50' 53.4408"	7° 15' 24.7500"
SN 26		Imo River – Okoloma	River	RVR 5	4° 51' 11.6640"	7° 13' 27.6132"
SN 27	**Egberu**	Ndoki Health Care Centre	Rain	HSP 2	4° 51' 07.6284"	7° 19' 06.1212"
SN 28		Ndoki Market	Rain	MKT 8	4° 50' 56.6016"	7° 19' 36.9012"
SN 29		Ndoki Comprehensive School	Rain	SCH 4	4° 50' 59.5212"	7° 19' 27.8616"
SN 30		Afam-Uku Settlement	Rain	SET 8	4° 49'	7° 19'

Sample Number	Study Axis	Sample Location	Sample Type	Sample ID	Coordinates	
					Latitude (N)	Longitude (E)
					00.0120"	00.0120"
SN 31		Egberu-Ndoki Settlement	Rain	SET 9	4° 48' 35.3562"	7° 16' 48.6335"
SN 32		Afam-Nta Settlement	Rain	SET 10	4° 48' 24.8508"	7° 20' 32.4888"
SN 33		Ban-Lori Market	Rain	MKT 9	4° 48' 22.7520"	7° 25' 55.2720"
SN 34		Obete Settlement	Rain	SET 11	4° 48' 39.4920"	7° 29' 14.0640"
SN 35	**Umu Agbai-Obete**	Umu Agbai Settlement	Rain	SET 12	4° 51' 12.3480"	7° 22' 38.5680"
SN 36		Okpontu Settlement	Rain	SET 13	4° 50' 05.7480"	7° 27' 31.8240"
SN 37		Azuagu Settlement	Rain	SET 14	4° 50' 51.3564"	7° 23' 35.3868"
SN 38		Marihun Settlement	Rain	SET 15	4° 50' 46.5900"	7° 25' 22.3824"
SN 39		Azumini Settlement	Rain	SET 16	4° 49' 07.4748"	7° 28' 29.6976"
SN 40		Imo River – Umu Agbai	River	RVR 6	4° 51' 27.9180"	7° 22' 19.8588"
SN 41		Imo River – Okpontu	River	RVR 7	4° 50' 35.8152"	7° 27' 01.5552"

2.2 Total Petroleum Hydrocarbon (TPH) Analysis

The assessment of TPH content in the water samples aimed to evaluate the concentrations of both petroleum aliphatic hydrocarbons and petroleum aromatic hydrocarbons present in the samples. For this purpose, Gas Chromatography Analysis was conducted using an Agilent 7820A gas chromatograph (GC) equipped with a flame ionization detector and an HP-5 fused silica capillary column (30m × 0.32 mm ID × 0.25 µm film thickness). The purified sample extracts underwent detailed analysis, employing helium as the carrier gas with a flow rate of 1.75 mL/min and an average velocity of 29.47 cm/sec. Injection occurred in splitless mode with a precisely measured 1 µL of the sample extract injected at a temperature of 300°C. The column temperature was initially set at 40°C for 1 minute, then increased at a rate of 7°C/min until reaching 320°C. The detector temperature was maintained at 300°C throughout the analysis, following the methodology outlined by Kim, Hong, and Won [28] and Inyang, Aliyu and Oyewale [29]. Calibration of the GC was performed using petroleum hydrocarbon calibration working standards prepared within the range of 0.05–20 µg/mL, with n-hexane as the diluent. Calibration curves were constructed, and average response factors for each analyte were generated using Agilent Chemstation chromatography software. These curves demonstrated linearity, with correlation coefficients ranging from 0.9846 to 0.9919. To quantify unresolved peaks, the response factor of nC-15 was employed following the approach outlined by Luan and Szelewski [30]. The determination of TPH content involved integration with baseline holding and peak sum slicing, encompassing the concentrations of n-alkanes eluting from nC-9 to nC-36, as well as the unresolved complex mixture (UCM). Data analysis utilized Agilent software to obtain ratios of low molecular n-alkanes to high molecular n-alkanes and unresolved n-alkanes to resolved n-alkanes, as elucidated by Inyang et al. [29]. This comprehensive analytical approach ensured accurate quantification and characterization of the total petroleum hydrocarbon content in the water samples.

2.3 Geospatial Pollutant Mapping

The concentrations of Total Petroleum Hydrocarbons (TPH) at each location were spatially represented using ArcGIS 10.4 software. This tool integrated the TPH analysis results of both rain and river water samples

collected from various sampling points in Oyigbo Local Government Area. The software processed these data as input variables, employing algorithms to generate graphical representations such as curves or contours, effectively illustrating the spatial distribution of water pollutant levels in the studied region.

3. RESULTS AND DISCUSSION

3.1 Total Petroleum Hydrocarbons (TPH) Distribution

To facilitate the analysis of total petroleum hydrocarbon (TPH) content variability in rain and water samples, the analyzed Total Aliphatic Hydrocarbons (TAH) encompassing C8 to C40, along with Pristane and Phytane, were strategically grouped into three classes for easier characterization. These categories and broad classification were adopted for this study based on the distinctive names and properties of individual hydrocarbons within each group, and providing a general categorization based on the number of carbon atoms in the molecular structure, although the properties of individual hydrocarbons within each group can vary based on factors such as branching and molecular arrangement [31].

The categorization of aliphatic hydrocarbons from C8 to C40 is undertaken with a focus on their molecular weight, recognizing that the weight of hydrocarbons increases with the number of carbon atoms. The adopted general grouping based on this study is structured as the Lighter Aliphatic Hydrocarbons (C8 to C16), with relatively lower molecular weights compared to their heavier counterparts. Medium Aliphatic Hydrocarbons (C17 to C24), including Pristane and Phytane, this group falls within the intermediate molecular weight range. Heavy Aliphatic Hydrocarbons (C25 to C40), consisting of hydrocarbons with higher molecular weights when contrasted with lighter aliphatic hydrocarbons [31].

Tables 4a, 4b, 4c, 4d, and 4e present a summary of the Aliphatic Hydrocarbon and Polycyclic Aromatic Hydrocarbon (PAH) contents in rain and river water samples from study locations. This presentation summarizes the maximum, minimum, and mean of TPH at distinct axes, offering an understanding of the hydrocarbon distribution within the studied environmental matrices.

Fig. 6a, 6b, 6c, 6d and 6e provide a detailed distribution chart of Aliphatic Hydrocarbon contents in rain and river water samples gathered from various locations based on the study axis. The X-axis of the chart corresponds to the sample locations and description, and the Y-axis displays the corresponding hydrocarbon concentrations.

Table 4a. TPH Content for Obigbo Study Axis (mg/L)

	Mean	Max	Min
C8 to C16	7.510	21.916	1.349
C17 to C24	14.940	25.780	6.665
C25 to C40	43.414	74.204	13.625
PAH	2.239	4.862	0.681

Table 4b. TPH Content for Komkom-Obiama Study Axis (mg/L)

	Mean	Max	Min
C8 to C16	0.486	5.511	2.324
C17 to C24	1.214	32.165	12.028
C25 to C40	7.103	26.720	18.984
PAH	0.459	2.878	1.581

Table 4c. TPH Content for Okoloma Study Axis (mg/L)

	Mean	Max	Min
C8 to C16	7.836	25.144	0.014
C17 to C24	15.010	24.897	1.417
C25 to C40	58.568	95.464	18.574
PAH	3.048	4.899	0.947

Table 4d. TPH Content for Egberu Study Axis (mg/L)

	Mean	Max	Min
C8 to C16	5.7305	12.77	0.097
C17 to C24	16.739	24.107	6.231
C25 to C40	20.789	56.027	4.982
PAH	1.531	3.687	0.568

Table 4e. TPH Content Umu Agbai-Obete Study Axis (mg/L)

	Mean	Max	Min
C8 to C16	1.480	8.275	0.1056
C17 to C24	7.223	22.862	1.497
C25 to C40	14.104	36.186	0.844
PAH	1.0167	2.591	0.241

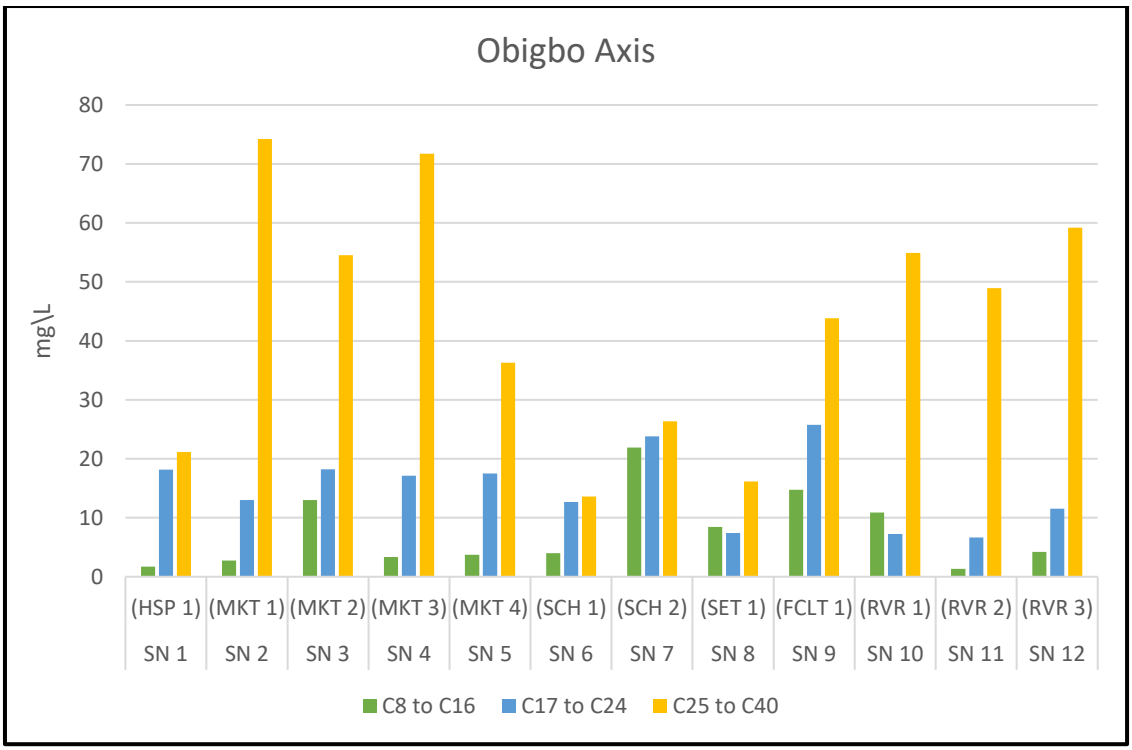

Fig. 6a. Aliphatic Hydrocarbons Distribution Chart for Obigbo Study Axis

The charts give a clear and depictive summary of the varying concentrations of TAH components and categories, offering an understanding of the hydrocarbon distribution within the studied environmental matrices. The components, classified into Light Aliphatic Hydrocarbons (C8 to C16) displayed by the green bar, Medium Aliphatic Hydrocarbons (C17 to C24, Pristane, and Phytane) represented with the blue bar, and Heavy Aliphatic Hydrocarbons (C25 to C40) indicated by the yellow-colored bar, reveal distinctive patterns and total concentration (mg/L) distributions for each sample across the study locations.

For C8 to C16 components, the highest concentrations were observed at SN 26 - RVR 5 (25.144 mg/L), SN 7 - SCH 2 (21.916 mg/L), SN 9 - FCLT 1 (14.746 mg/L), SN 28 - MKT 8 (12.77 mg/L), SN 20 - MKT 7 (10.964 mg/L), and SN 10 - RVR 1 (10.879 mg/L). Lower concentrations in this category between 30 mg/L to 10 mg/L values were generally scattered across different samples with SN 31 - SET 9 (0.097 mg/L), SN 30 - SET 8 (0.98 mg/L), and SN 21 - SET 5 (0.721 mg/L) being the lowest distribution with values below 10 mg/L concentration.

In the C17 to C24 range, SN 18 - RVR 4 (32.165 mg/L), SN 23 - SET 7 (24.897 mg/L), SN 29 -

SCH 4 (24.107 mg/L), SN 25 - FCLT 3 (23.004 mg/L), SN 41 - RVR 7 (22.862 mg/L), SN 27 - HSP 2 (20.838 mg/L), SN 26 - RVR 5 (22.444 mg/L), and SN 20 - MKT 7 (20.322 mg/L), displayed the highest values, while various samples exhibited concentrations between 20 mg/L to 5 mg/L. The lowest concentration distributions in the medium TAH components were recorded at SN 38 - SET 15 (1.497 mg/L), SN 21 - SET 5 (1.417 mg/L), and SN 17 - SET 4 (1.214 mg/L). For C25 to C40 components, SN 20 - MKT 7 (93.966 mg/L), SN 25 - FCLT 3 (88.131 mg/L), SN 26 - RVR 5 (87.464 mg/L), SN 2 - MKT 1 (74.204 mg/L) and SN 4 - MKT 3 (71.756 mg/L) showed the highest concentrations, with distributions in values between 70 mg/L and 10 mg/L across different samples, while the lowest values were recorded at SN 17 - SET 4 (7.103 mg/L), SN 31 - SET 9 (5.005 mg/L), SN 35 - SET 12 (3.464 mg/L), and SN 36 - SET 13 (0.844 mg/L).

Examining Pristane concentrations, the peaks were observed at SN 19 - MKT 6 (2.885 mg/L), SN 22 - SET 6 (2.852 mg/L), SN 16 - SET 3 (2.623 mg/L), SN 29 - SCH 4 (2.62 mg/L), SN 18 - RVR 4 and SN 26 - RVR 5 at 2.107 mg/L, SN 13 - MKT 5 (1.836 mg/L), and SN 5 - MKT 4 (1.724 mg/L). Conversely, the lowest values were observed in SN 31 - SET 9 (0.059 mg/L), SN 8 - SET 1, SN 15 - SET 2, SN 17 - SET 4, also SN 37 - SET 14 recorded concentrations of 0.42 mg/L, while SN 35 - SET 11 has no presence of Pristane. For Phytane concentrations distribution, SN 25 - FCLT 3 (1.400 mg/L), SN 7 - SCH 2 (2.320 mg/L), SN 8 - SET 1 (1.487 mg/L) and SN 15 - SET 2 at 2.487 mg/L represented the highest value. Several locations across the study area recorded Phytane distribution values within the ranges of 1.0 mg/L to 0.1 mg/L, while SN - MKT 1, SN 31 - SET 9, SN 32 - SET 10, SN 33 - MKT 9, and SN 36 - SET 13 presented no presence of Phytane.

In the comprehensive assessment of the entire study area and specific axes, it is evident that the concentration and distribution of hydrocarbon components in the C25 to C40 range are the highest, followed by C17 to C24, while the least distribution is observed in the C8 to C16 range. Within the Obigbo Axis, MKT 1 exhibits the highest distribution, followed by MKT 3, with SCH 1 displaying the least distribution. In the Komkom-Obiama Axis, RVR 4 and SET 3 demonstrate the highest distribution, while SET 4 displays the least distribution. Moving to the Okoloma Axis, RVR 7, MKT 7, and FCLT 3 represent the highest distribution, while SET 5 reflects the least distribution. In the Egberu Axis of the study, HSP 2 exhibits the highest distribution, whereas SET 8 and SET 9 display the least distribution.

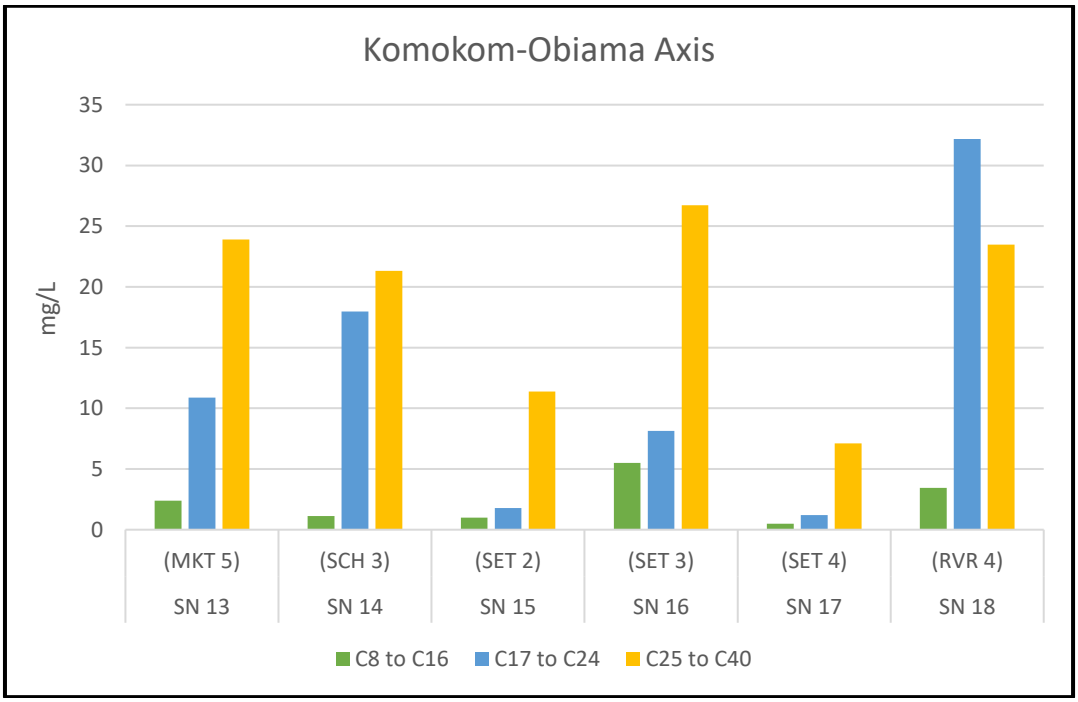

Fig. 6b. Aliphatic Hydrocarbons Distribution Chart for Komkom-Obiama Study Axis

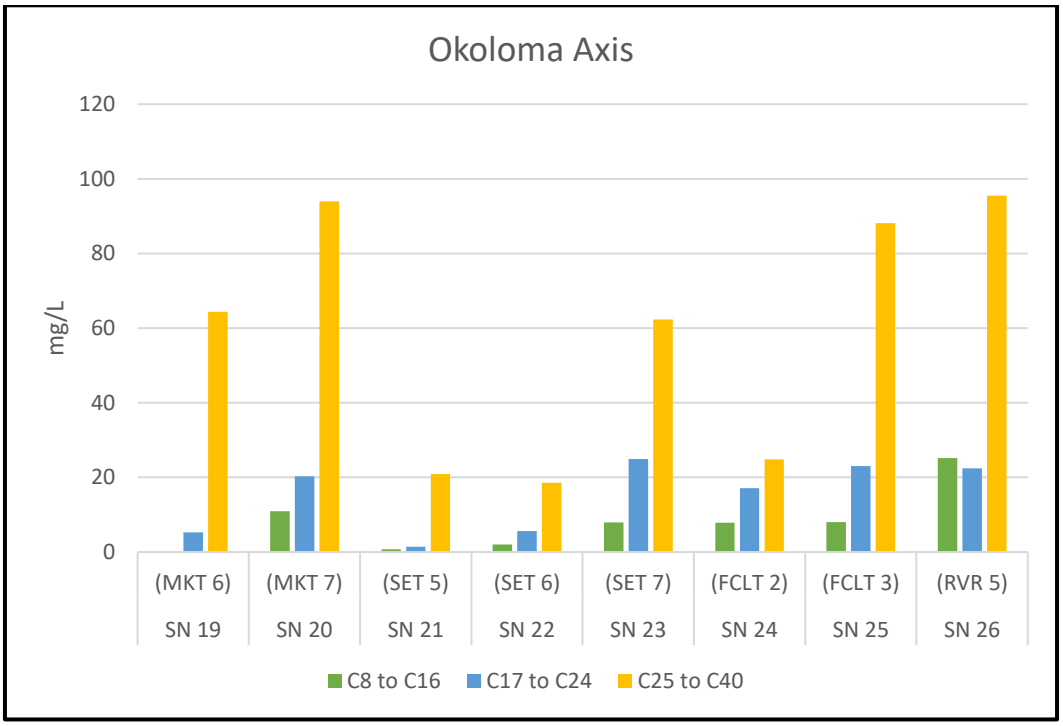

Fig. 6c. Aliphatic Hydrocarbons Distribution Chart for Okoloma Study Axis

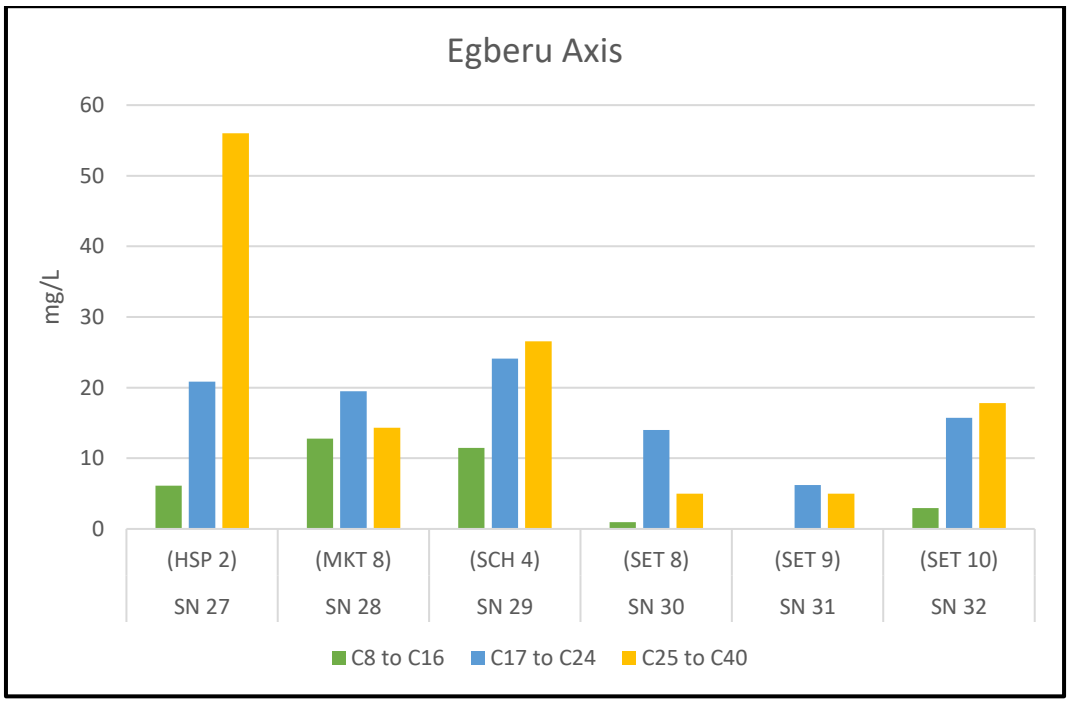

Fig. 6d. Aliphatic Hydrocarbons Distribution Chart for Egberu Study Axis

Notably, the Umu Agbai-Obete Axis stands out as the area with the least distribution of Aliphatic Hydrocarbons across all locations studied. Within this axis, RVR 7 has the highest concentration, while SET 12, and SET 13 represent the least Total Aliphatic Hydrocarbon (TAH) distributions. These detailed findings provide valuable insights into the spatial variations of hydrocarbon components, emphasizing specific areas with elevated concentrations and others with lower distribution within the studied regions and axes.

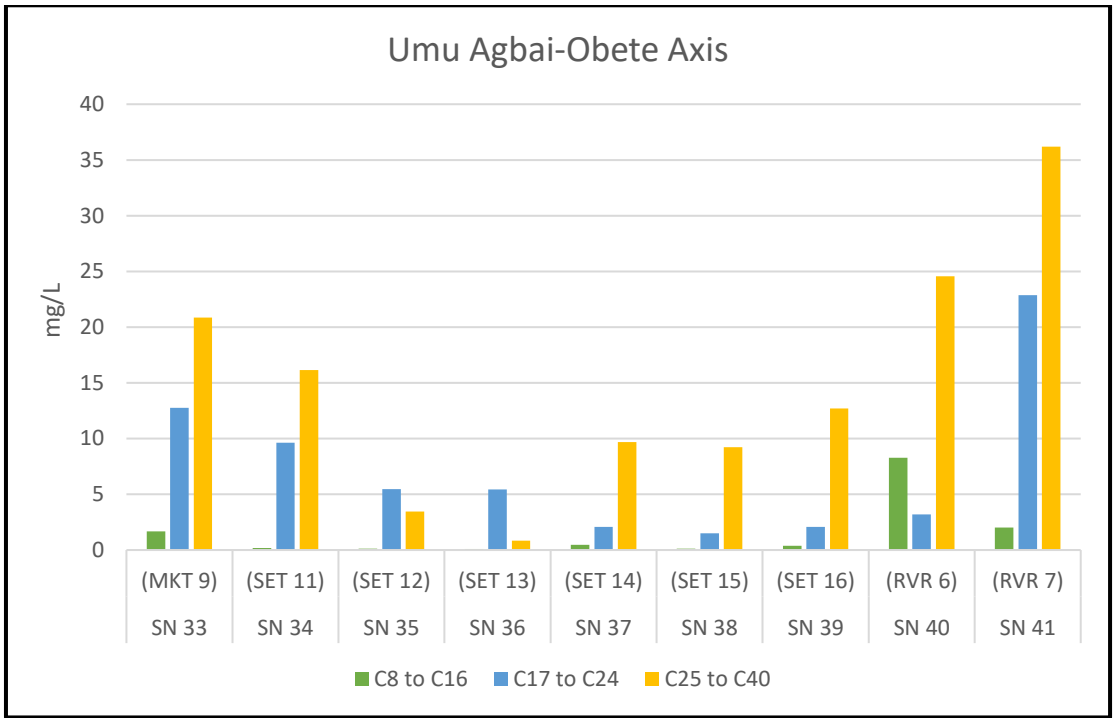

Fig. 6e. Aliphatic Hydrocarbons Distribution Chart for Umu Agbai-Obete Study Axis

Overall, in the rainwater samples, the Total Aliphatic Hydrocarbons (TAH) exhibited its highest concentration, reaching 128.197 mg/L at location 20 (MKT 7), while the lowest value, recorded at 8.976 mg/L, was observed at location 36 (SET 13). Meanwhile, in the river water samples, the maximum TAH value of 137.397 mg/L was noted at location 26 (RVR 5), and the minimum, at 37.118 mg/L, was recorded at location 40 (RVR 6). These categorizations provide a clear understanding of hydrocarbon distribution patterns across different aliphatic components in the sampled locations, providing valuable insights into the pollution intensity and potential sources of hydrocarbon contamination in the study area and emphasizing the need for a comprehensive understanding of hydrocarbon distribution across the sampled locations for effective environmental assessment.

The distributions of Polycyclic Aromatic Hydrocarbon (PAH) components in various samples collected from distinct locations, generally has most of the sample falling below 1.0 mg/L concentrations with only 12 samples above the value. Fig. 7a, 7b, 7c, 7d, and 7e illustrate the comprehensive distribution chart for the entire Polycyclic Aromatic Hydrocarbon (PAH) components. The distribution is depicted hierarchically, presenting the values in a ring format to facilitate a comparative analysis of the concentration proportions across distinct hierarchical levels. Anthracene reached the highest concentration at SN 10 - RVR 1 (0.410 mg/L), and SN 41 - RVR 7 (0.210 mg/L). Pyrene exhibited its highest concentration at SN 4 - MKT 3 (0.271 mg/L), while multiple samples had no detectable levels. Chrysene concentrations were highest at SN 5 - MKT 4 (0.359 mg/L), with several samples containing no detectable levels.

Fluoranthene concentrations peaked at SN 2 - MKT 1 (1.180 mg/L), while multiple samples showed no presence. Benzo [a] Anthracene displayed its highest concentration at SN 30 - SET 3 (0.370 mg/L). Benzo [b] Fluoranthene concentrations were highest at SN 32 - SET 10 (1.042 mg/L), and SN 5 - MKT 4 (1.0 mg/L), while multiple samples had no detectable levels. Benzo [k] Fluoranthene exhibited its highest concentration at SN 24 - FCLT 3 (1.254 mg/L), SN 22 - SET 6 (1.043 mg/L), and SN 21 - SET 5 (1.032 mg/L) with various samples containing no detectable levels. Benzo [a] Pyrene reached its highest concentration at SN 13 - MKT 5 (1.270 mg/L), SN 1 - HSP 1 (1.050 mg/L), and SN 15 - SET 2 (1.001 mg/L), while multiple samples showed no presence. Indenol [1,2,3, cd] pyrene concentrations peaked at SN 9 - FCLT 1 (1.103 mg/L), SN 5 - MKT 4 (1.059 mg/L), SN 16 - SET 3 (1.050 mg/L), SN 36 - SET 13, and SN 24 - FCLT 2 at 1.00 mg/L, with multiple samples containing no detectable levels.

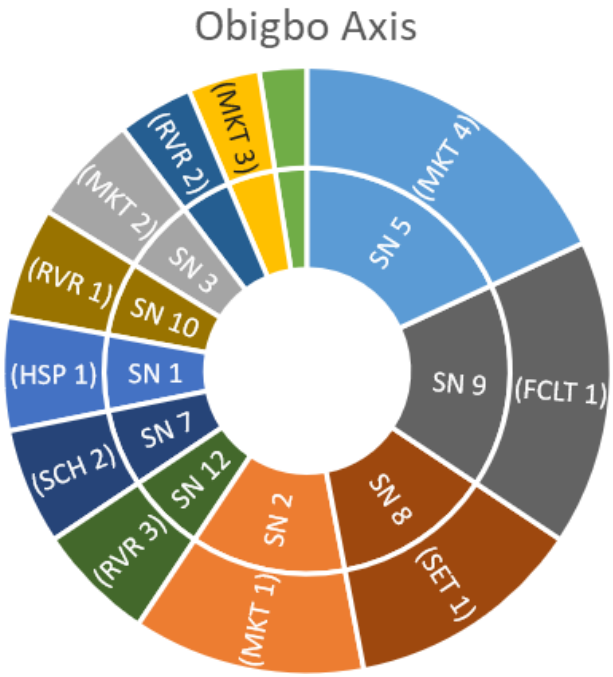

Fig. 7a. PAH Distribution Chart for Obigbo Study Axis

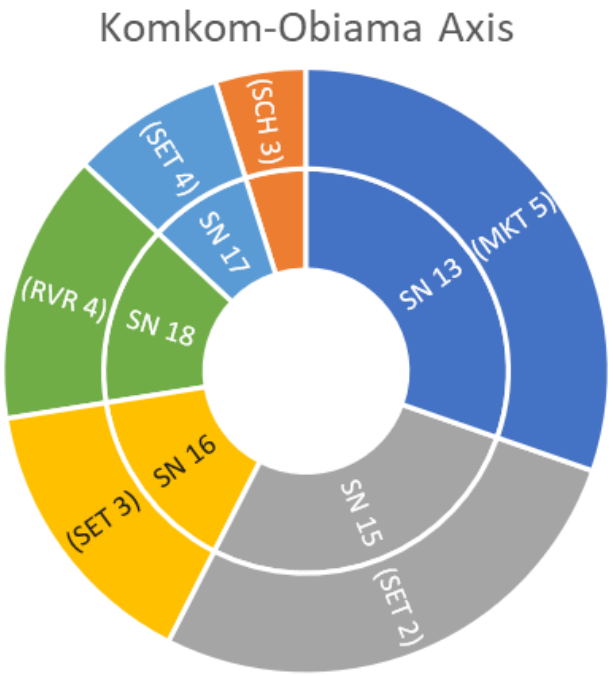

Fig. 7b. PAH Distribution Chart for Komkom-Obiama Study Axis

Dibenzo [a,h] Anthracene recorded the highest concentration distributions in all the PAH components with highest value at SN 24 - FCLT 2 (2.211 mg/L), while multiple samples showed concentrations above 1.0 mg/L. The PAH distributions across various study axes exhibit consistent trends, showcasing distinct regions with higher concentrations sharing similar contamination levels. Conversely, areas with lower concentrations display analogous levels, as evident in the charts.

In the Obigbo Axis, four locations, MKT 4, FCLT 1, SET 1, and MKT 1, comprise most PAH

concentrations, covering over half of the distribution across the axis. The remaining eight locations represent less than half of the distribution, with SCH 1 exhibiting the lowest concentration in the axis. Similarly, the Komkom-Obiama Axis demonstrates comparable trends, where two locations, MKT 5 and SET 2, carry most PAH concentrations, while the remaining four locations, SET 3, RVR 4, SET 4, and SCH 3, represent less than half of the distribution in the axis. In the Okoloma Axis, three locations, FCLT 2, SET 5, and SET 6, account for more than half of the distribution, leaving the remaining five locations with concentrations below half of the overall levels.

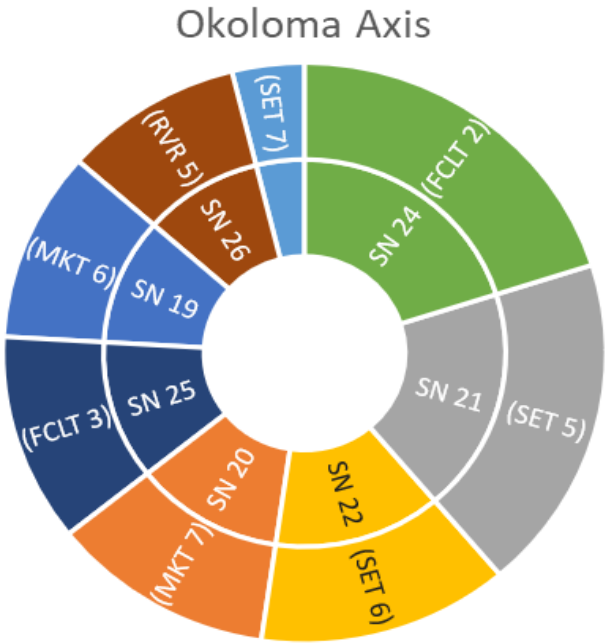

Fig. 7c. PAH Distribution Chart for Okoloma Study Axis

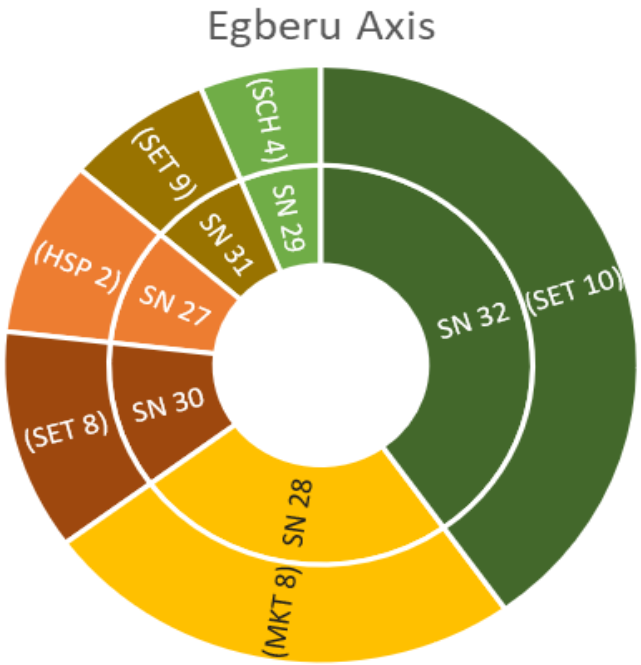

Fig. 7d. PAH Distribution Chart for Egberu Study Axis

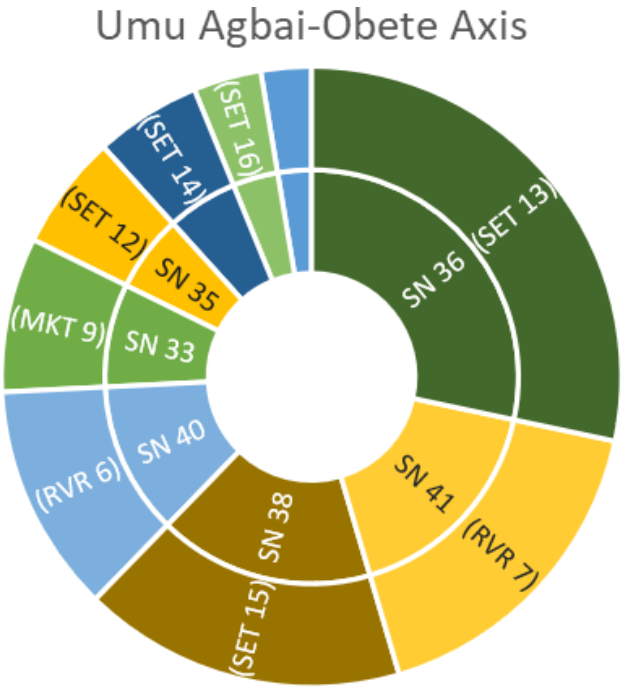

Fig. 7e. PAH Distribution Chart for Umu Agbai-Obete Study Axis

Moving to the Egberu Axis, two locations, SET 10 and MKT 8, occupy two-thirds of the entire region, while the remaining four locations, SET 8, HSP 2, SET 9, and SCH 4, share the rest of the distribution. In the Umu Agbai-Obete Axis, nine locations are observed, with three of them, SET 13, RVR 7, and SET 15, occupying more than half of the distribution in the region. The remaining six locations, SET 15, RVR 6, MKT 9, SET 12, SET 14, and SET 11, have lower concentrations, with SET 11 having the least levels. Generally, Naphthalene, Methylnaphthalene, Acenaphthylene, Acenaphthene, Fluorene, and Phenanthrene components consistently exhibited the lowest PAH availability and distribution, with concentrations below 1.0 mg/L, and in several instances, reaching undetectable The overall concentration of PAHs reached its peak at SN 24 - FCLT 2 (4.899 mg/L), SN 5 - MKT 4 (4.862 mg/L), and SN 21 - SET 5 (4.56 mg/L). Notably, SN 34 - SET 11 and SN 39 - SET 16 recorded the lowest PAH concentrations, at 0.241 mg/L and 0.324 mg/L, respectively.

Fig. 8 provides a clear visualization of the distribution of Total Petroleum Hydrocarbon (TPH) concentrations across all river and rainwater samples collected from various locations within the Oyigbo Local Government Area. The figure distinctly portrays the varying levels of TPH contaminations, showcasing a hierarchical occurrence pattern. SN 26 (RVR 5) emerges as the location with the highest TPH concentration, recording 137.397 mg/L. In close succession, SN 20 (MKT 7) follows with a substantial TPH concentration of 128.179 mg/L. Conversely, SN 36 (SET 13) registers the lowest TPH concentration in the figure, indicating 8.976 mg/L.

This presentation effectively illustrates the diverse distribution of petroleum hydrocarbon contamination across the entire study area. Additional samples with medium to high TPH concentrations include SN 12 (RVR 3) at 76.676 mg/L, and SN 2 (MKT 1), SN 9 (FCLT 1), SN 19 (MKT 6), SN 23 (SET 7), ranging from 100 mg/L to 70 mg/L. Samples showing average TPH concentrations include SN 18 (RVR 4), SN 19 (MKT 6), SN 29 (SCH 4), SN 41 (RVR 7), SN 23 (SET 17), SN 24 (FCLT 2), with concentrations ranging from 70 mg/L to 50 mg/L. Samples with average to lower TPH concentrations include SN 14 (SCH 3), SN 32 (SET 10), SN 22 (SET 6) ranging within 40 mg/L to 20 mg/L. Samples displaying relatively lowest TPH concentrations are SN 15 (SET 2), SN 30 (SET 8), SN 31 (SET 9) with concentrations ranging from between 20 mg/L to 10 mg/L, and SN 36 (SET 13), SN 35 (SET 12), and SN 17 (SET 4) records the least TPH concentration at 8.976 mg/L, 9.613 mg/L, and 9.583 mg/L respectively.

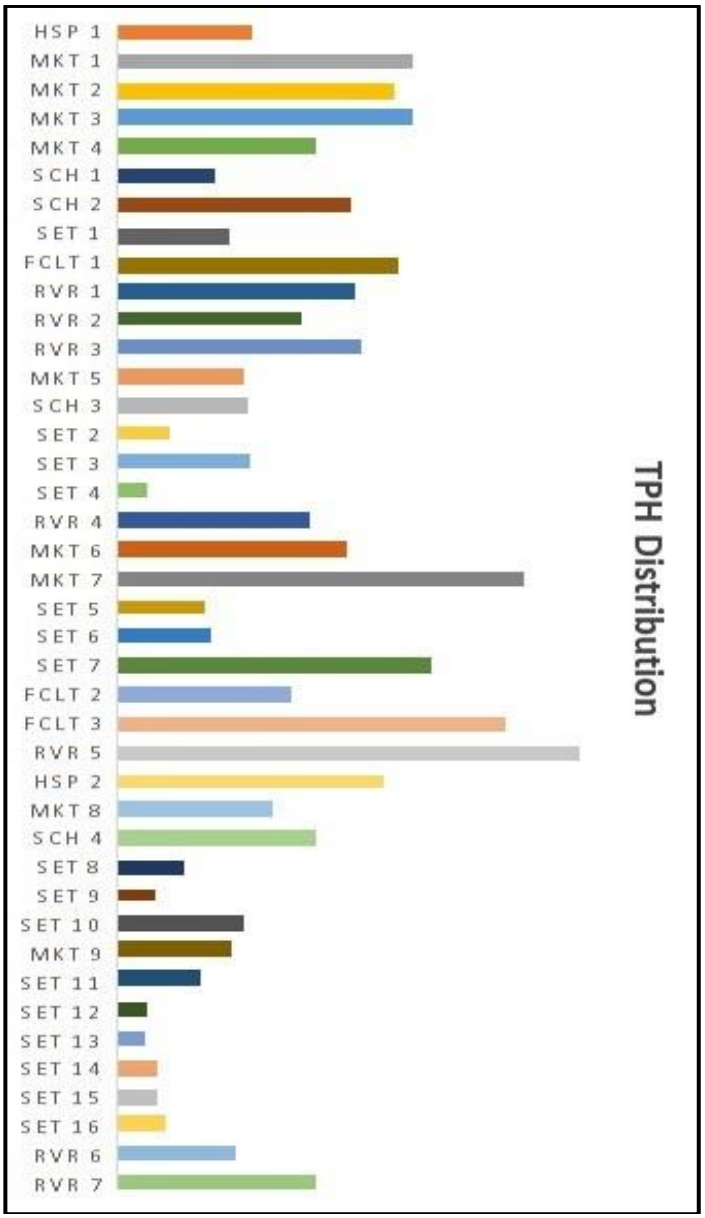

Fig. 8. TPH Distribution Chart for Rain and River Water Samples across the Study Area

3.2 Total Petroleum Hydrocarbon (TPH) Geospatial Variation

Fig. 9a to 9h illustrate the spatial variation maps of the Aliphatic Hydrocarbon components across the study area, Fig. 9i depicts the spatial variation maps for Total Aliphatic Hydrocarbon (TAH), and Polycyclic Aromatic Hydrocarbon (PAH), while Fig. 9j shows the spatial variation of the Total Petroleum Hydrocarbons (TPH). The analysis of hydrocarbons with smaller chain lengths (C8 to C17) consistently revealed low concentrations, depicted by light coloration in the mapped area. Conversely, long-chain hydrocarbons from C18 to C40 and Pristane displayed an even distribution across the study area without distinct hotspots. Phytane, however, exhibited higher concentrations in the western part of the study area and lower values in the eastern part (Fig. 9h). Spatial maps illustrated significant variation, with lighter colors indicating lower values in the southern parts and localized hotspots indicating higher hydrocarbon concentrations, particularly along the Imo River channel in the northern part (Fig. 9i and 9j).

In assessing the geospatial variations of C6 to C11 and C12 to C15 Aliphatic Hydrocarbon components (Fig. 9a and 9b) across the study area, heightened concentrations were identified,

particularly in the western and central regions. Notably, for C8 to C15 components, significant concentrations were observed at specific locations such as Imo River - Obiama and Okoloma areas in the Komkom-Obiama, and Okoloma axis respectively, Community Secondary School, Umuakpahu and Obigbo Market area in the Obigbo axis, and Umuosi Market area in the Okoloma axis. The concentration peaks in these areas, represented by a darker color intensity on the map, signify substantial pollution levels in the specified locations. Conversely, lower variations in this category were predominantly observed in the eastern regions, particularly at Azuagu, Obete, and Okpontu settlement areas, all situated in the Umu Agbai-Obete axis, displaying lighter color intensity on the map, and indicating comparatively lower pollution levels in these areas.

Within the C16 to C21 and C22 to C25 ranges, as illustrated in Fig. 9c and 9d, a noticeable intensification in concentration is prominently observed in the northwestern and north-central parts of the study area, depicted by the deep coloration on the map. The mapping distinctly reveals heightened pollution levels in key locations, notably in the Umuosi area, Imo River, Otamiri River, Komkom area, Umuebele area in the Obigbo, Komkom-Obiama, and Okoloma axes of the study. Conversely, the southern region of the study area consistently displays lower concentrations, evident from the lighter color intensities, particularly in the Ban-Lori and Ndoki areas within the Egberu and Umu Agbai-Obete axes. The substantial variations between these regions of high and low pollution intensity underscore the significant disparities in contamination levels.

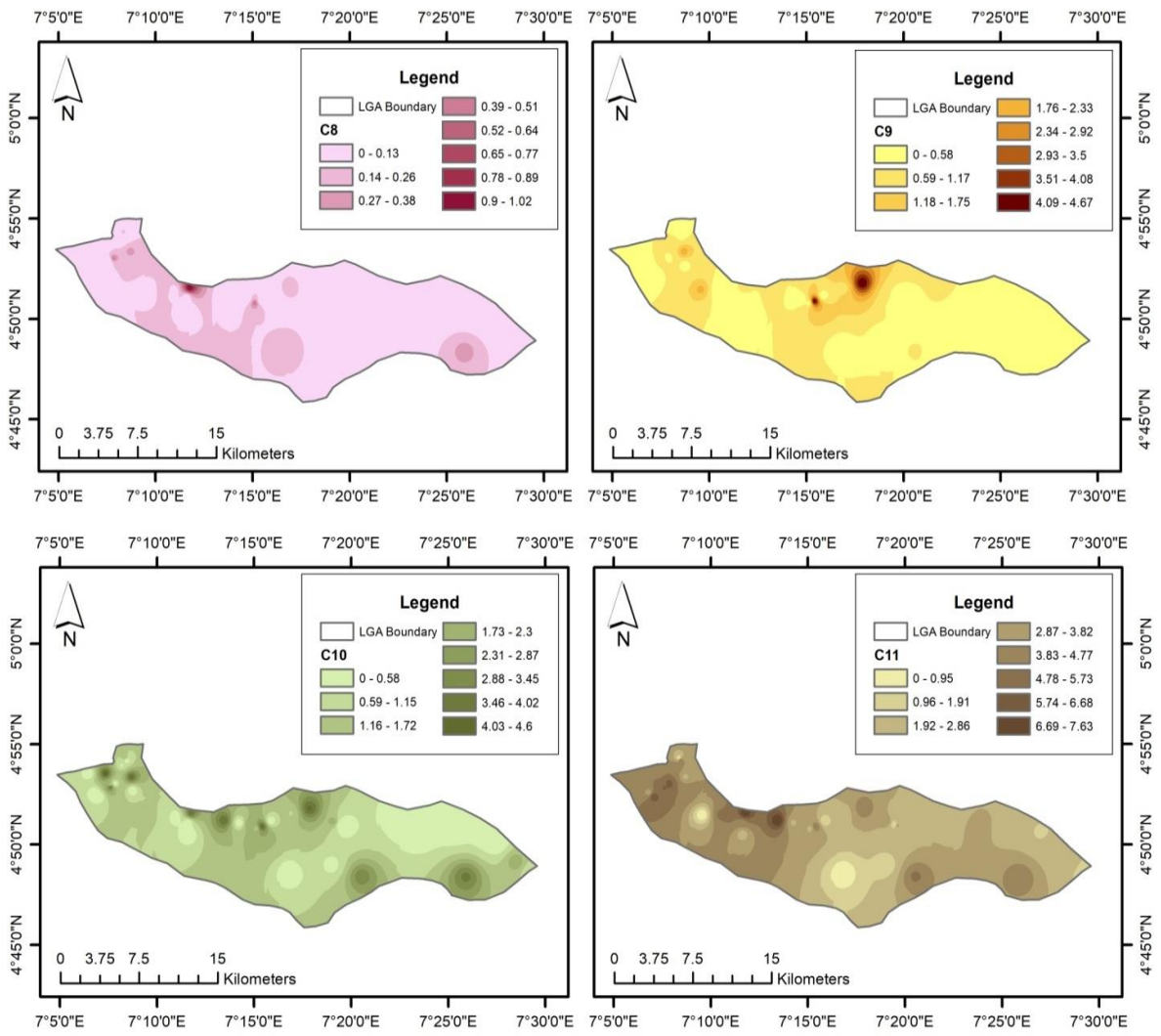

Fig. 9a. Spatial variations of C_8 to C_{11} Aliphatic Hydrocarbon contents across the Study Area

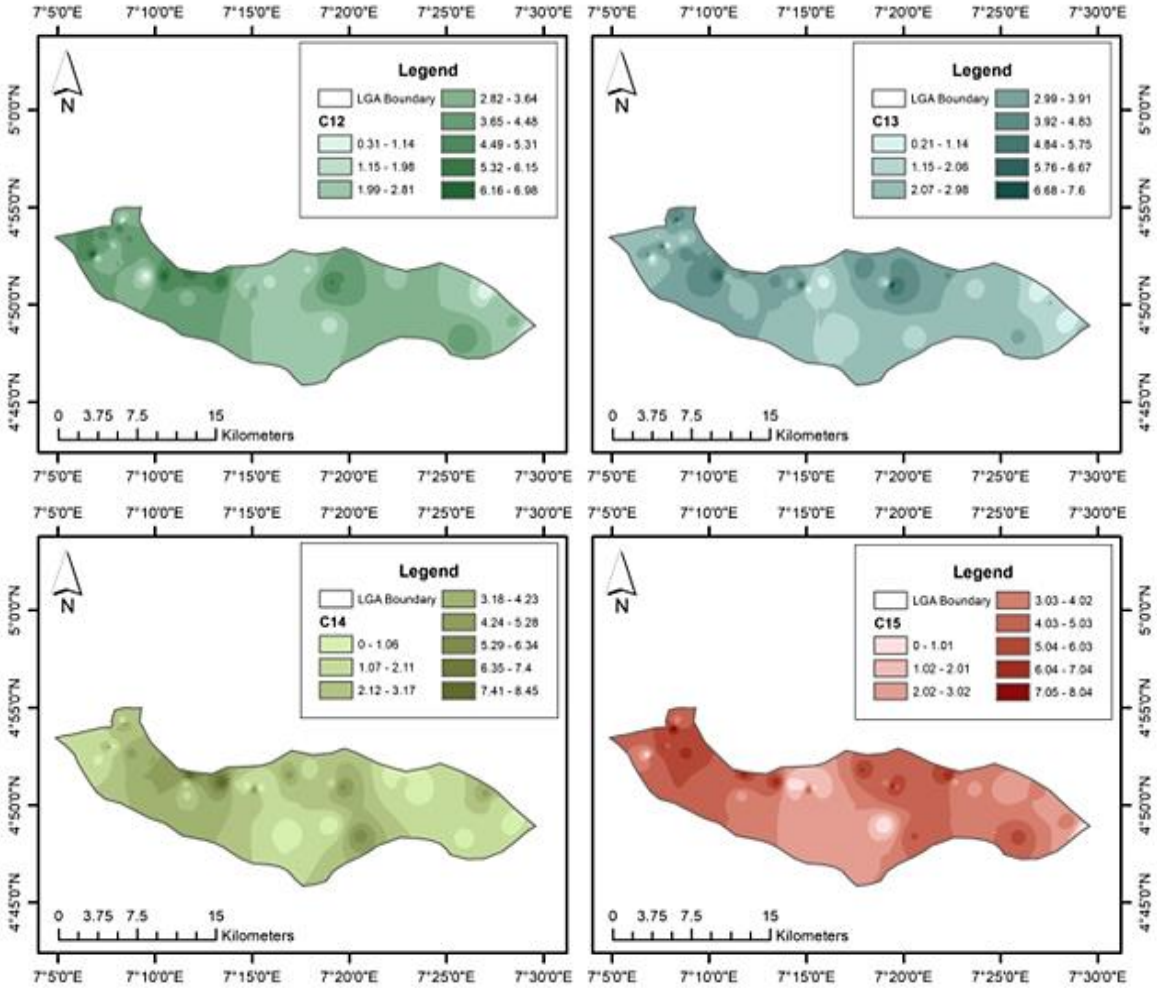

Fig. 9b. Spatial variations of C_{12} to C_{15} Aliphatic Hydrocarbon contents across Study Area

In the context of C26 to C31 and C32 to C35 components, as depicted in Fig. 9e and 9f, the spatial variation maps reveal heightened pollution concentrations primarily in the northern regions of the study area, consistently portrayed by deep color intensities. The areas exhibiting elevated pollution levels are predominantly in the Umuosi area and Imo River area within the Okoloma axis of the study. Additionally, contaminated zones, as indicated by the spatial variation map, include the Timber Market and Atata Market areas, both situated in the Obigbo axis. In contrast, a lesser intensity of contamination is observed in the southern strip and eastern regions of the study area, particularly around the Obigbo-Etche boundary regions, Umu Agbai, Egberu, and Obete areas. The spatial distribution underscores the close proximity of these high pollution areas to the location of oil and gas production facilities in the Obigbo and Okoloma regions.

For C36 to C39 components (Fig. 9g), the spatial variation map reveals a comparatively lower contamination intensity of these components compared to others across the entire study area. There is a moderate dispersion and variation of the C36 to C39 components, as indicated by predominantly light-colored regions throughout the study area. Specific location-bound hotspots are observed at two points, with Umuosi, Imo River, Timber Market, and Atata Market areas in the Obigbo and Okoloma axis displaying higher pollution levels. Overall, these components exhibit a medium contamination intensity, as suggested by the average color tone covering the majority of the study area. The areas with the lowest pollution are depicted by very light colors on the map, primarily located at the Umu Agbai and Obete axis of the study.

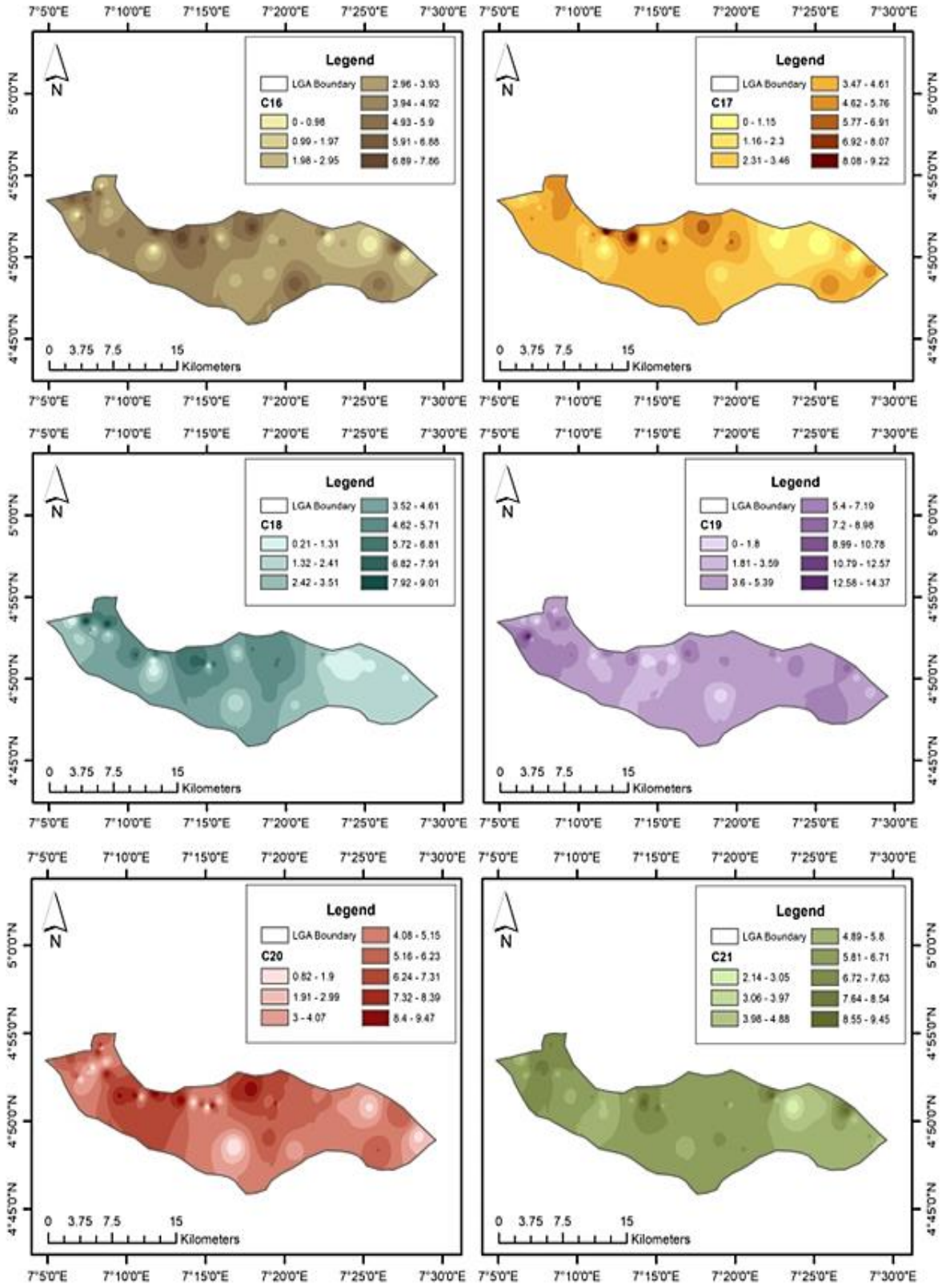

Fig. 9c. Spatial variations of C_{16} to C_{21} Aliphatic Hydrocarbon contents across the Study Area

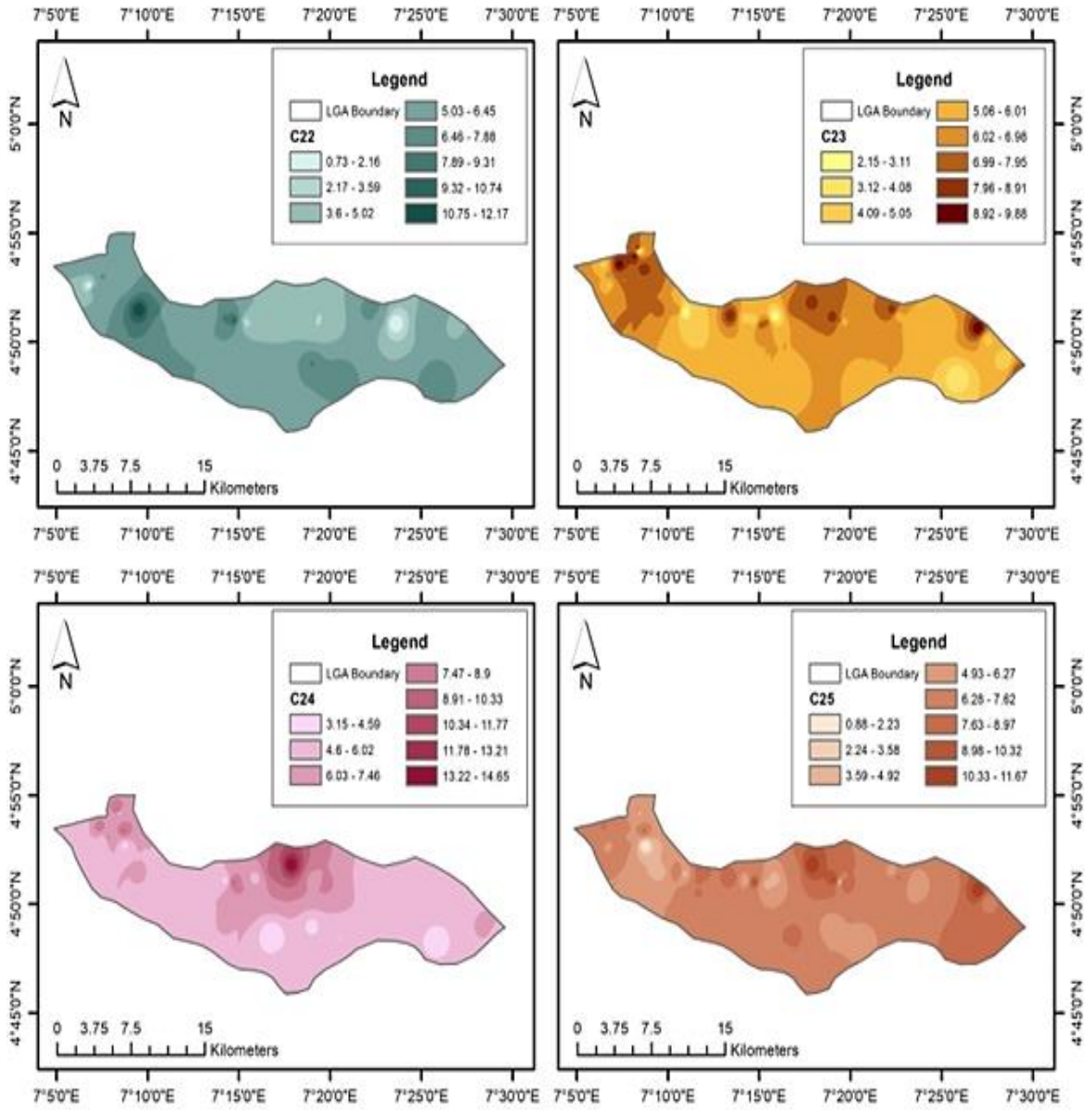

Fig. 9d. Spatial variations of C_{22} to C_{25} Aliphatic Hydrocarbon contents across Study Area

In Fig. 9h, the geospatial variations for C40, Pristane, and Phytane components of the Aliphatic Hydrocarbons are depicted. Upon examining C40 and Phytane concentrations, a similar pollution dispersion pattern is observed, evident in the color-coding style across the study area. These components exhibit heightened pollution in the North-central and North-western regions, with medium pollution extending from these zones towards the Southwestern to Central parts. The peaks are primarily concentrated around the Shell Flow Station, and Afam Power Plant, in the Obigbo and Okoloma axis, indicating a significant deposition of the heavier C40 components around the sources of contamination. Conversely, lesser pollution dispersion is observed around the Komkom, Ka Lori, and Obete areas, while average pollution dispersion is displayed in the Obiama and Egberu areas. For Pristane, high pollution concentrations are distributed across major regions, illustrating a well-distributed spatial variation throughout the study area in the Obigbo, Komkom-Obiama, Okoloma, Egberu, and parts of the Umu Agbai-Obete axis.

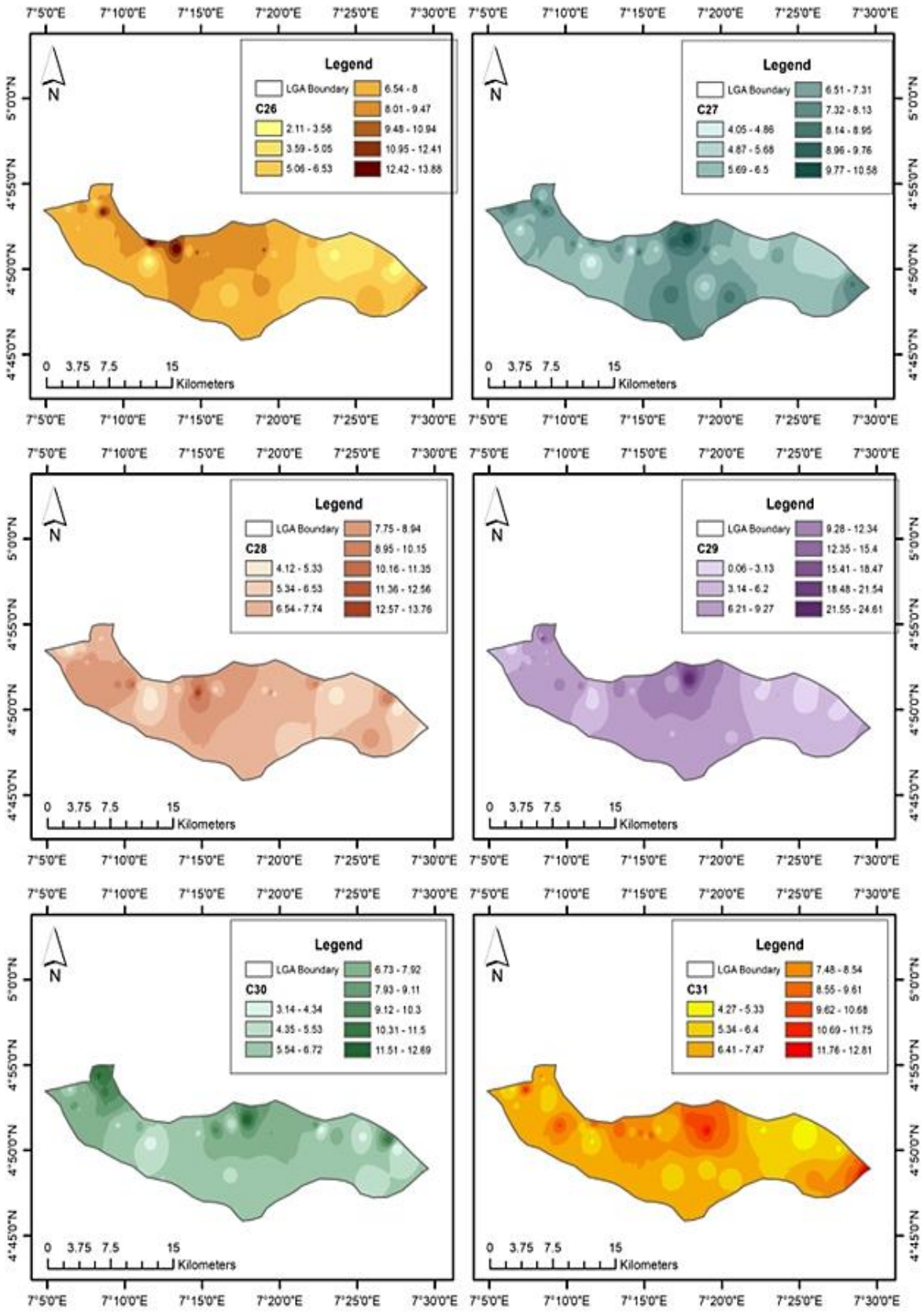

Fig. 9e. Spatial variations of C_{26} to C_{31} Aliphatic Hydrocarbon contents across the Study Area

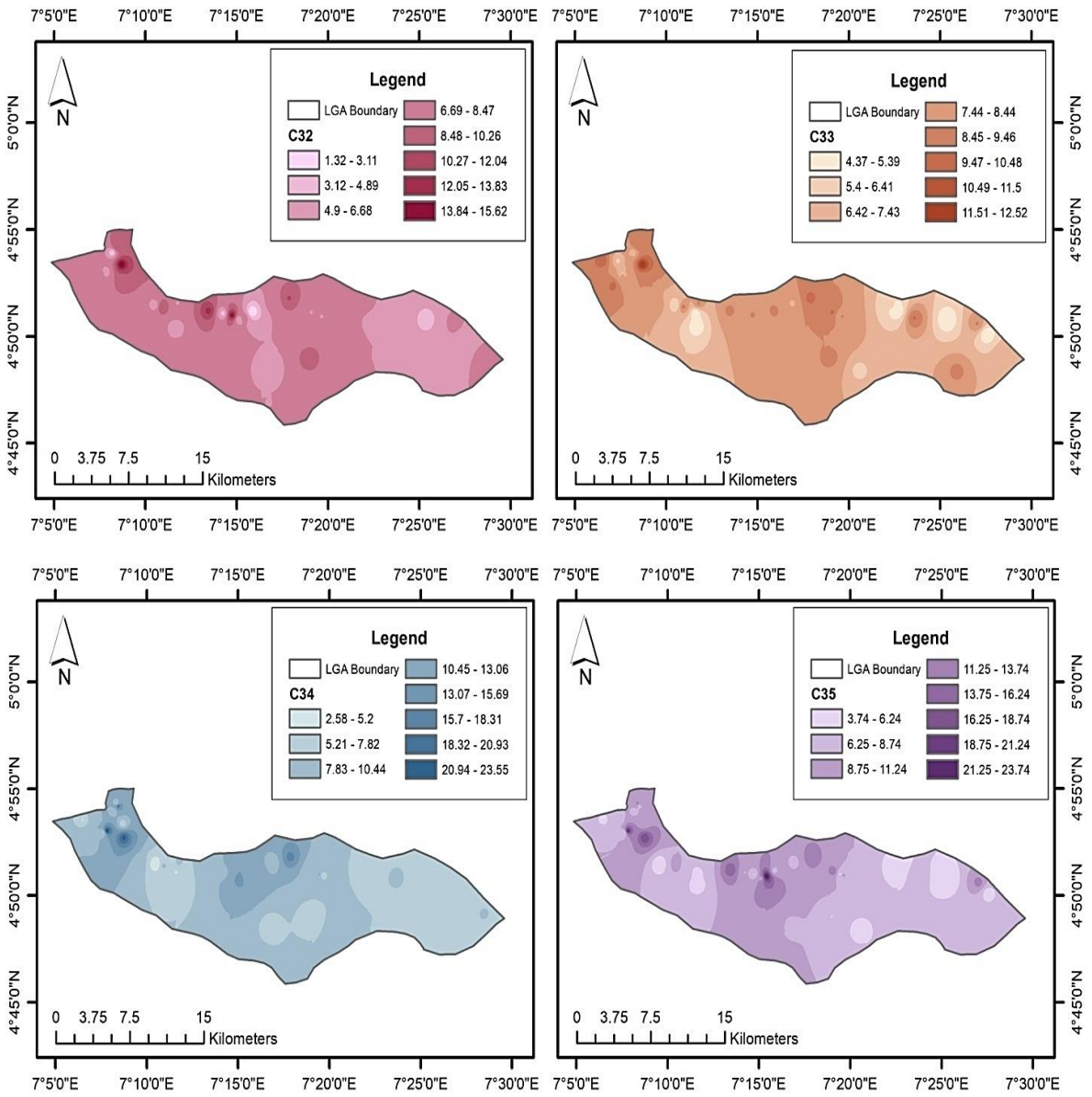

Fig. 9f. Spatial variations of C_{32} to C_{35} Aliphatic Hydrocarbon contents across the Study Area

In general, the Aliphatic Hydrocarbons registered its heightened pollution levels at locations including RVR 5, MKT 3, MKT 6, MKT 7, SET 7, and SCH 2, corresponding to Imo River, Atata Market, Okoloma Market, Umuosi Market, Afam area, and Community Secondary School, Umuakpahu, located in the Okoloma, Obiama, and Obigbo study locations and axes. Conversely, the least pollution intensities were observed at SET 4, SET 8, SET 9, SET 12, SET 13, and SET 15, situated in Obiama Settlement area, Afam-Uku Settlement areas, Egberu-Ndoki Settlement area, Umu Agbai Settlement area, Okpontu Settlement area, and Marihun Settlement areas, within the Obiama, Egberu, and Umu Agbai-Obete study axis.

The overall concentration of Polycyclic Aromatic Hydrocarbons (PAH) prominently heightened in the Northern, North-western, and South-central locations, specifically at MKT 4, SCH 1, SET 5, SET 6, MKT 6, and FCLT 2. Conversely, SET 3, SET 8, SET 9, MKT 8, MKT 9, SET 11, SET 12, and SET 16 recorded the lowest PAH concentrations. These areas with lower pollution levels are primarily situated in Komkom, Egberu, Umu Agbai, and Obete, spanning the Western, Central, and Eastern regions of the study area.

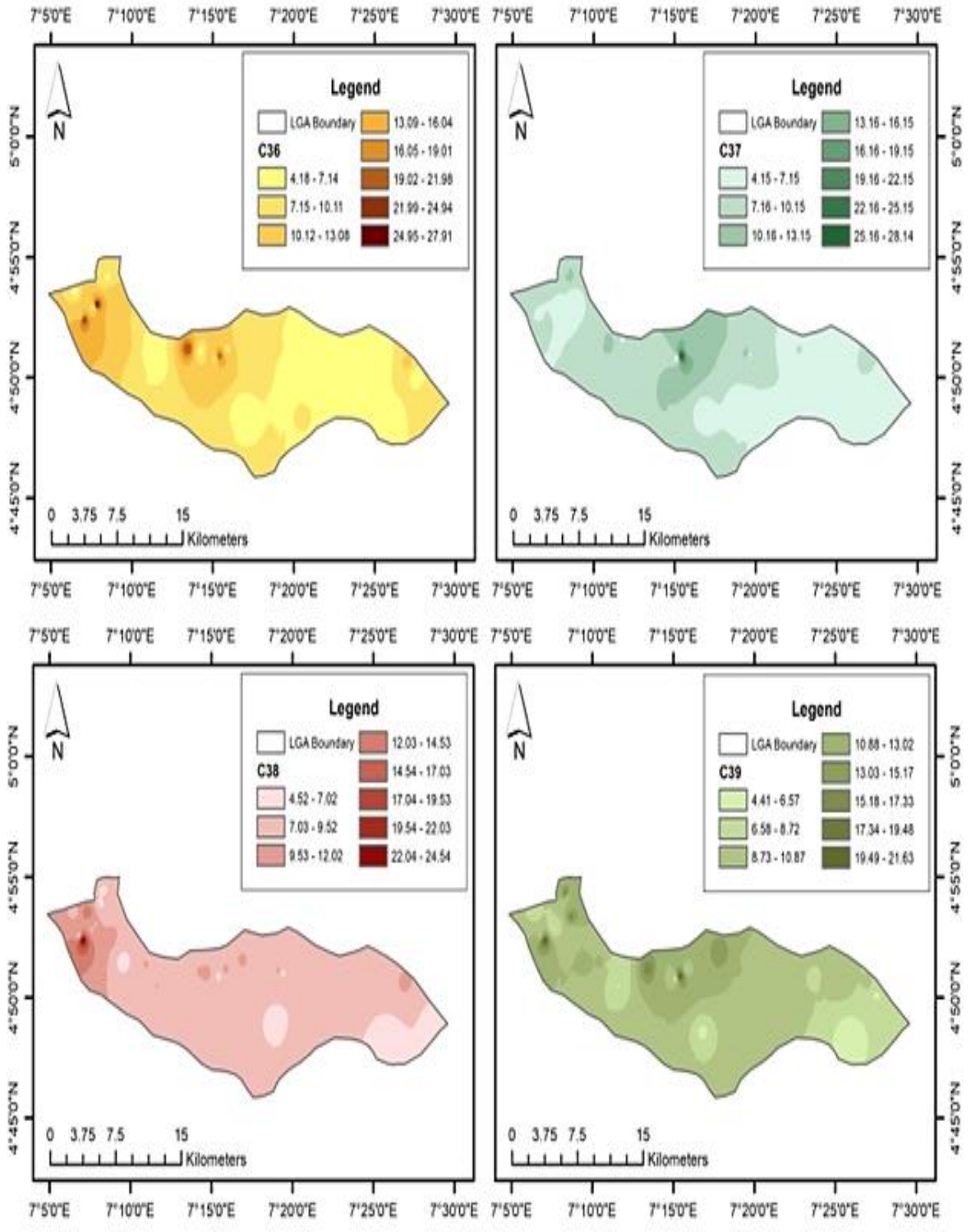

Fig. 9g. Spatial variations of C_{36} to C_{39} Aliphatic Hydrocarbon contents across the Study Area

Overall, the Total Petroleum Hydrocarbon (TPH) demonstrates its highest pollution dispersion in the North-central and North-western regions of the study area, with a generally medium dispersion more prevalent across the Central and Southern regions. The lowest pollution is predominantly displayed in the Eastern regions, evident in corresponding TPH concentrations and differences in color intensities. Specifically, the Umuosi, Obumku, and Imo River areas in the

Okoloma axis, as well as the Umuebele areas in the Obigbo axis, exhibit the highest pollution levels, while the lowest pollution is observed at Obiama Settlement areas in the Obiama region, Egberu-Ndoki Settlement areas in the Egberu axis, and Marihun and Okpontu Settlement areas in the Umu Agbai-Obete axis of the study area.

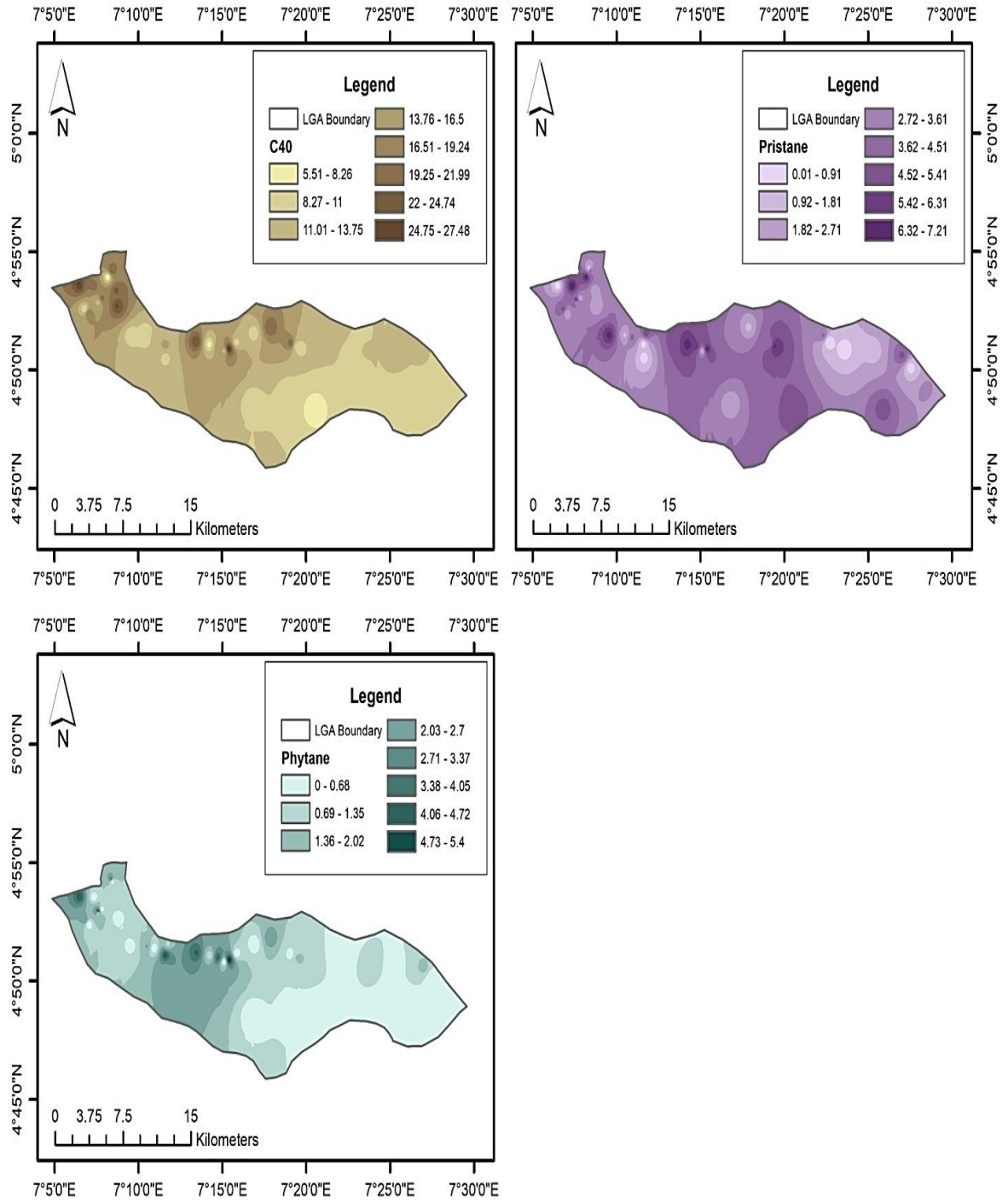

Fig. 9h. Spatial variation of C_{40}, Pristane and Phytane Aliphatic Hydrocarbon across Study Area

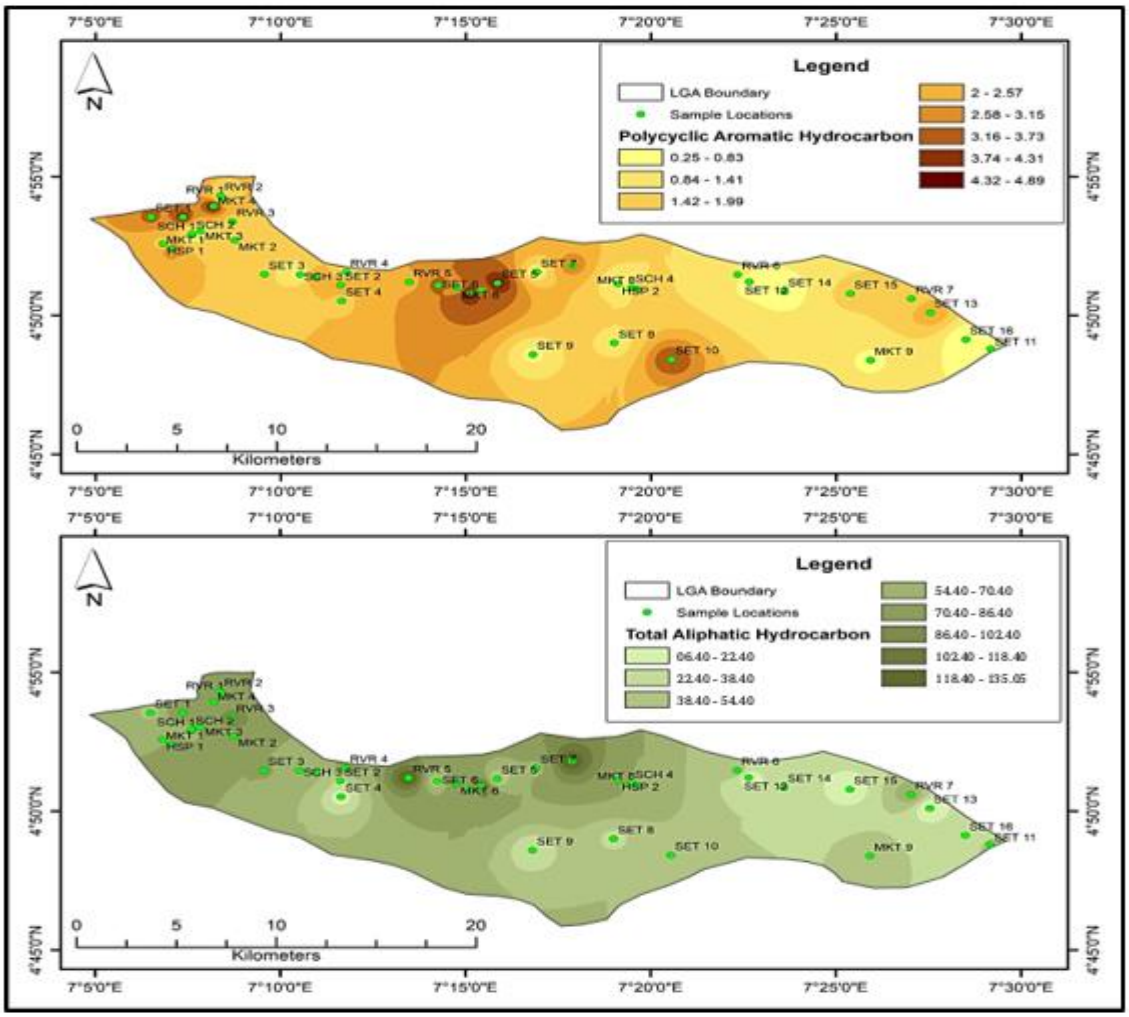

Fig. 9i. Spatial Variation of Aliphatic Hydrocarbons and PAH across Study Area

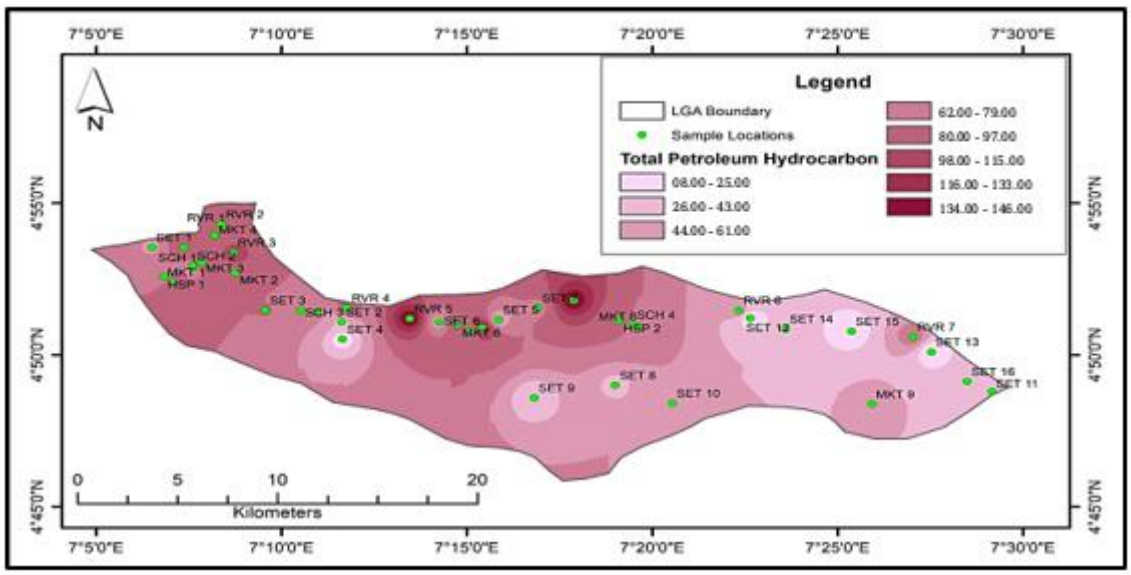

Fig. 9j. Spatial Variation of Total Petroleum Hydrocarbon (TPH) across the Study Area

4. CONCLUSION

This study provides a thorough examination of Total Petroleum Hydrocarbon (TPH) concentrations in rain and rivers affected by soot contamination in Oyigbo, Rivers State, Niger Delta, Nigeria. The research focuses on understanding the geospatial variability and distribution of TPH, with a specific emphasis on Aliphatic Hydrocarbons and Polycyclic Aromatic Hydrocarbons (PAHs), aiming to identify pollution hotspots and vulnerable areas.

The investigation categorizes hydrocarbons based on chain lengths and components, revealing consistent concentrations of Lighter Aliphatic Hydrocarbons at specific locations. However, variations are observed in Medium and Heavy Aliphatic Hydrocarbons, and distinct patterns emerge in Pristane and Phytane concentrations across locations. Out of the 41 samples, 19 locations exceeded the 50 mg/L acceptable limits set by the World Health Organization [32] and the Department of Petroleum Resources [33]. Additionally, 10 locations recorded concentrations above, while 12 locations fell below 30 mg/L. These results indicate that approximately 46% exhibited high, 24% displayed medium, and 29 % showcased low concentrations across the study area. The study highlights the highest pollution dispersion in the North-central and North-western regions, with medium dispersion more prevalent in the Central and Southern regions. The Eastern regions consistently display the lowest pollution levels, particularly in Obiama, Egberu-Ndoki, and Marihun-Okpontu Settlement areas. Conversely, higher pollution levels are likely linked to proximity to major petroleum production facilities in the Okoloma and Obigbo axes.

Exposure to TPH in soot-contaminated rain and river water poses potential human health risks, including respiratory issues and skin irritations. Additionally, consumption of contaminated water can contribute to respiratory problems and gastrointestinal disorders [34]. Ecologically, TPH contamination disrupts aquatic ecosystems, harming fish, invertebrates, and organisms throughout the food chain [31]. Urgent intervention is required through enhanced monitoring, remediation efforts, and strict regulatory measures. Sustainable water management practices are crucial for minimizing the impact of TPH contamination on human health and ecosystems. The study's findings contribute valuable insights for environmental sustainability in Oyigbo, emphasizing the need for a holistic approach to address hydrocarbon contamination. Increased monitoring, remediation, and regulatory efforts are necessary to mitigate the impact on water resources and surrounding ecosystems [35].

COMPETING INTERESTS

Authors have declared that no competing interests exist.

REFERENCES

1. Adeyeye JA, Akintan OB, Adedokun T. Physicochemical characteristics of harvested rainwater under different rooftops in Ikole Local Government Area, Ekiti State, Nigeria. Journal of Applied Sciences and Environmental Management. 2019;23(11):2003-2008
2. Akudinobi BEB, Chibuzor SN. Hydrochemical evaluation of water sources in Warri metropolis, Delta State, Nigeria. Journal of Basic Physical Research. 2012; 3:64-72.
3. Samuel P, Elechi O, Julius NE. Total Hydrocarbon Contents: Spatial Variations in Aquatic Environment of Oyigbo Communities, Rivers State. International Journal of Environmental Protection and Policy. 2022;10(1):1-5.
4. Anornu GK, Kabo-bah AT, Anim-Gyampo M. Evaluation of groundwater vulnerability in the Densu River basin of Ghana. American Journal of Human Ecology. 2012;1(3):79-86.
5. Ahmed NO, Diepiriye CO, Chinemerem PE. Geochemical assessment of hydrocarbon contaminated site in central Niger Delta, Nigeria. International Journal of Research. 2019; 6(6):505-520.
6. Okorhi-Damisa FB, Ogunkeyede AO, Akpejeluh P, Okechukwu L. Analysis of soot in rainwaters around Warri metropolis. International Journal of Scientific Development and Research. 2020; 5(5): 319-325.
7. Zabbey N, Sam K, Newsom CA, Nyiaghan PB. The COVID-19 lockdown: An opportunity for conducting an air quality baseline in Port Harcourt, Nigeria. The Extractive Industries and Society. 2021; 8(1):244-256.
8. Anslem OA. Negative effects of gas flaring: the Nigerian experience. Journal of

Environment Pollution and Human Health. 2013;1(1):6-8.
9. Chen D, Guo Z. The Source, Transport, and Removal of Chemical Elements in Rainwater in China. Sustainability. 2022; 14(19):12439.
10. Olowoyo DN. Physicochemical characteristics of rainwater quality of Warri axis of Delta state in western Niger Delta region of Nigeria. Journal of Environmental Chemistry and Ecotoxicology. 2011; 3(12):320-322.
11. Jiang XQ, Mei XD, Feng D. Air pollution and chronic airway diseases: what should people know and do? Journal of Thoracic Disease. 2016;20(1):31-40.
12. Antai RE, Osuji LC, Obafemi AA, Onojake MC. Air quality changes and geospatial dispersion modeling in the dry season in Port Harcourt and its Environs, Niger Delta, Nigeria. International Journal of Environment, Agriculture and Biotechnology. 2018;3(3):882-898.
13. Manisalidis I, Stavropoulou E, Stavropoulos A, Bezirtzoglou E. Environmental and health impacts of air pollution: a review. Frontiers in public health. 2020;8:14.
14. Moore CC, Corona J, Griffiths C, Heberling MT, Hewitt JA, Keiser DA, Kling CL, Massey DM, Papenfus M, Phaneuf DJ, Smith DJ, Wheeler W. Measuring the social benefits of water quality improvements to support regulatory objectives: Progress and future directions. Proceedings of the National Academy of Sciences. 2023;120 (18):e2120247120.
15. Fawole OG, Cai XM, MacKenzie AR. Gas flaring and resultant air pollution: A review focusing on black carbon. Environmental pollution. 2016;216:182-197.
16. American Institute for Conservation of Historic and Artistic Works (AICHAW). The hidden hazards of fire soot; 2010. Available:https://www.culturalheritage.org/docs/defaultsource/publications/periodicals/newsletter/2010-09-sept-aicnews.pdf. [Accessed December 21, 2023].
17. Weisman W. Analysis of petroleum hydrocarbons in environmental media. In total petroleum hydrocarbon criteria working group (TPHCWG) Series: vol. 1. Weisman, W.Ed. Amherst Scientific Publishers, Amherst, MA. 1998;1-98.
18. Bakhtiari AR, Zakaria MP, Yaziz MI, Lajis MNH, Bi X. Polycyclic aromatic hydrocarbons and nalkanes in suspended particulate matter and sediments from the Langat river, Peninsular Malaysia. Environ. Asia. 2009;2:1-10.
19. NBS National Bureau of Statistics – Nigeria: Social Statistics Report; 2006.
20. Samuel P, Elechi O, Julius NE. Total Hydrocarbon Contents: Spatial Variations in Aquatic Environment of Oyigbo Communities, Rivers State. International Journal of Environmental Protection and Policy. 2022;10(1):1-5.
21. Onwuka C, Eboatu AN, Ajiwe VIE, Morah EJ. Pollution studies on soils from crude oil producing areas of rivers state, Niger delta region, Nigeria. Open Access Library Journal. 2021;8(9):1-17.
22. Adejuwon JO. Rainfall seasonality in the Niger delta belt, Nigeria. Journal of Geography and Regional Planning. 2012; 5(2):51.
23. Okorafor GF, Okoronkwo C, Oladejo E. Infrastructure Development and Maintenance in the Oil Producing Areas of Southern Nigeria: Implications Options and Challenges. Fepnek Synergy Journal. 2017;30.
24. Abhulimhen B. Physico-Chemical Properties of Soil Sourced from Automobile Mechanic Workshop in Ikoku Mechanic Village, Mile 3 Diobu, Port Harcourt, Rivers State, Nigeria; 2016. Available:https://dx.doi.org/10.2139/ssrn.3490585
25. Fagorite VI, Ahiarakwem CA, Okeke OC, Onyekuru SO. Physico-chemical characteristics of otamiri river and its sediments in parts of Owerri. Elixir Geology. Elixir International Journal. 2019; 131:53223-53229.
26. Enotoriuwa RU, Nwachukwu EO, Ugbebor JN. Assessment of particulate matter concentration among land use types in Obigbo and environs in rivers state Nigeria. International Journal of Civil Engineering and Technology. 2016; 7(3):252-261.
27. Okorie DO, Nwosu PO. Seasona Variations in Physico-Chemical of Imo River. Journal of Pharmacy and Biological Sciences. 2014;9(5):07-09.
28. Kim M, Hong SH, Won J. Petroleum hydrocarbon contaminations in the intertidal seawater after the Hebei Spirit oil spill-effect of tidal cycle on the TPH concentrations and the chromatographic

characterization of seawater extracts. Wat. Res. 2013;47:758-768.
29. Inyang SE, Aliyu AB, Oyewale AO. Total petroleum hydrocarbon content in surface water and sediment of Qua-Iboe River, Ibeno, Akwa-Ibom State, Nigeria. Journal of Applied Sciences and Environmental Management. 2018;22(12):1953-1959.
30. Luan W, Szelewski M. Ultra-fast total petroleum hydrocarbons (TPH) analysis with Agilent low thermal mass (LTM) GC and simultaneous dual-tower injection. Agilent Technologies Application Note: Environmental. 2008;1-8.
31. Omokpariola DO, Nduka JK, Kelle HI, Mgbemena NM, Iduseri EO. Chemometrics, health risk assessment and probable sources of soluble total petroleum hydrocarbons in atmospheric rainwater, Rivers State, Nigeria. Scientific Reports. 2022;12:11829.
Available:https://doi.org/10.1038/s41598-022-15677-7
32. WHO Guidelines for drinking-water quality Fourth edition incorporating the first addendum, Geneva, Switzerland: World Health Organization; 2017.
Available:http://apps.who.int/iris/bitstream/10665/254637/1/9789241549950-eng.pdf?ua=1. [Assessed Dec 2, 2023].
33. Department of Petroleum Resources (DPR). Environmental Guidelines and Standards for the Petroleum Industry in Nigeria (EGASPIN) (Third Edition); 2018.
Available:https://pdfcoffee.com/dpregaspin-2018-pdf-free.html. [Accessed January 29, 2024].
34. Orji D, Ndu A, Ihesinachi K, Adaunwo EO. The total petroleum hydrocarbon contents of the ambient air within Port Harcourt and environs. Chemistry Research Journal. 2019;4(3):117-123.
35. NPC. National Population Commission: 2006 Population and Housing Census of the Federal Republic of Nigeria; 2006.

Peer-review history:
The peer review history for this paper can be accessed here:
https://www.sdiarticle5.com/review-history/113182